


 Cite this: *RSC Adv.*, 2024, 14, 13291

Syntheses, structural, photophysical and theoretical studies of heteroleptic cycloplatinated guanidinate(1–) complexes bearing acetylacetonate and picolinate ancillary ligands†

 Vasudha Thakur,^a Jisha Mary Thomas,^b Mohammad Adnan,^c Chinnappan Sivasankar,^b G. Vijaya Prakash^c and Natesan Thirupathi^{*a}

Cycloplatinated of symmetrical N,N',N'' -triarylguanidines, $(ArNH)_2C=NAr$ with cis -[Pt(TFA)₂(S(O)Me₂)₂] in toluene afforded cis -[Pt(TAG)(TFA)(S(O)Me₂)₂] (TAG = triarylguanidinate(1–)-κC,κN; TFA = OC(O)CF₃; **6–9**) in 75–82% yields. The reactions of **6–9** and the previously known cis -[Pt(TAG)X(S(O)Me₂)₂] (X = Cl (**1**) and TFA (**2–5**)) with acetylacetonate (acacH) or 2-picolinic acid (picH) in the presence of a base afforded [Pt(TAG)(acac)] (acac = acetylacetonate-κ²O,O'; **10–18**) and [Pt(TAG)(pic)] (pic = 2-picolinate-κN,κO; **19**) in high yields. The new complexes were characterised by analytical, IR and multinuclear NMR spectroscopies. Further, molecular structures of **11**, **12**, **13**·0.5 toluene and **14–19** were determined by single crystal X-ray diffraction. Absorption spectra of **10–19** in solution and their emission spectra in crystalline form were measured. Platinacycles **10–19** are bluish green light emitter in the crystalline form, and emit in the λ_{PL} = 488–529 nm range (**11** and **13–19**) while **12** emits at λ_{PL} = 570 nm. Unlike other platinacycles, the emission band of **12** is broad, red shifted, and this pattern is ascribed to the presence of an intermolecular N–H⋯Pt interaction involving the endocyclic amino unit of the six-membered [Pt(TAG)] ring and the Pt(II) atom in the adjacent molecule in an asymmetric unit of the crystal lattice. Lifetime measurements were carried out for all platinacycles in crystalline form, which revealed lifetime in the order of nanoseconds. The origin of absorption and emission properties of **11**, **15**, **18** and **19** were studied by TD-DFT calculations.

Received 1st February 2024

Accepted 14th April 2024

DOI: 10.1039/d4ra00828f

rsc.li/rsc-advances

Introduction

Cycloplatinated nitrogen donor complexes that contain one or two Pt–C(aryl) bonds are known for their intriguing structural, bonding, photophysical properties and biological applications.¹ Heteroleptic complexes [Pt(ND)(acac)] (ND = Monoanionic nitrogen donor ligands-κC,κN; acac = acetylacetonate-κ²O,O' (**A**)) and [Pt(ND)(pic)] (pic = 2-picolinate-κN,κO (**B**)) are a well-studied class of cycloplatinated nitrogen donor complexes due to their interesting structural, bonding and emission properties (see Fig. 1). The availability of a range of 2-arylpyridyl type nitrogen donor ligands for cycloplatinated reaction, tunability

of substituents on both the chelate rings in **A** and **B** makes this class of complexes as suitable substrates for structural and photophysical studies.^{2–14} The photophysical properties such as color purity, quantum yield, Φ_{PL} and life time of the excited state, τ of complexes of the types **A** and **B** were changed by tuning the substituent on either of the chelate rings. Further, this type of platinacycles were shown to act as metal-lobesogens¹⁵ and as O₂ sensors.^{16–19}

The strongly σ-donating aryl carbon and π-accepting nitrogen atom of the C,N chelate ring in **A** and **B** were shown to widen the d–d energy gap so that the non-radiative decay of excited state is minimized. Other structural features such as geometry of the platinum, degree of steric encumbrance around the Pt(II) atom, substitution pattern and conjugation in the chelate rings and degree of non-covalent interactions in the crystal lattice were shown to influence the photophysical properties of these complexes significantly. It has been suggested that platinacycles with rigid scaffolds are desirable for developing luminescent materials with high quantum yield, Φ_{PL}.^{1f} The square planar geometry of the Pt(II) atom in sterically unencumbered **A** permits aggregation in the crystal lattice through Pt⋯Pt and π–π interactions thereby leading to the

^aDepartment of Chemistry, University of Delhi, Delhi 110 007, India. E-mail: tnat@chemistry.du.ac.in; thirupathi_n@yahoo.com

^bDepartment of Chemistry, Catalysis and Energy Laboratory, Pondicherry University, Puducherry 605 014, India. E-mail: siva.che@pondiuni.edu.in

^cDepartment of Physics, Nanophotonics Laboratory, Indian Institute of Technology-Delhi, New Delhi 110 016, India. E-mail: prakash@physics.iitd.ac.in

 † Electronic supplementary information (ESI) available: XYZ files containing the coordinates of the DFT optimised species and TD-DFT related data. CCDC 1887641–1887649. For ESI and crystallographic data in CIF or other electronic format see DOI: <https://doi.org/10.1039/d4ra00828f>

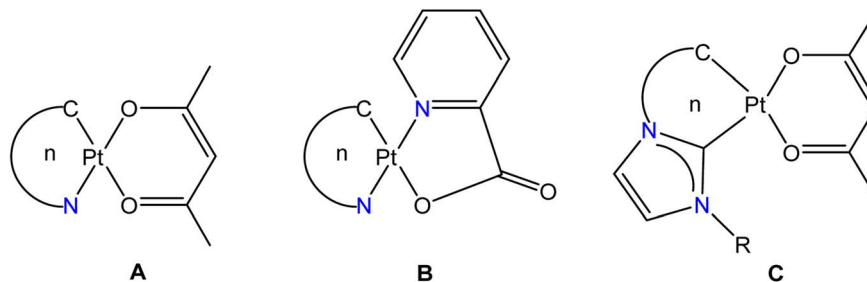



Fig. 1 Types of heteroleptic cycloplatinated nitrogen- and carbon-donor complexes known in the literature. The letter *n* refers to the ring size of the [Pt(ND)] (ND = monoanionic nitrogen donor ligand- κ C, κ N; (A and B)) and [Pt(CD)] (CD = monoanionic carbon donor ligand- κ^2 C,C'; (C)) units.

formation of excimer and thus influences the shape and wavelength of emission bands.^{13b,20,21} A detailed theoretical calculations have been carried out on type A complexes to understand the origin of emission, band shapes and structure-emission property relationship.²²

Cycloplatinated carbon donor complexes derived from imidazoles such as C are studied due to the presence of strongly σ -donating carbene carbon, which rises the energy of non-radiative d-d states on the metal center thereby increasing the energy spacing with emissive excited states and thus improving the quantum yield, Φ_{PL} . The presence of a stable M-C_{carbene} bond in C could increase the lifetime of these materials in organic electronic devices.^{23,24} Five-membered platinacycles of the types A and B are well-known ($n = 5$) while to the best of our knowledge only two six-membered platinacycles A ($n = 6$) and none of the type B ($n = 6$) are known in the literature.^{25,26}

The C,N chelate rings in A and B are usually derived from a rigid nitrogen donor ligands such as 2-arylpyridyls. We wanted to utilize a range of triarylguanidinate(1⁻) ligand as monoanionic C,N chelate ring in A and B to investigate whether the resulting heteroleptic complexes are emissive or non-emissive. Further, we wanted to tune the substituents in the aryl rings in the C,N chelate of A and B to investigate whether this endeavor has any influence on the structural and photophysical properties of these complexes.

The photophysical properties of cycloplatinated imino(1⁻) complexes are sparsely studied in the literature.²⁷⁻²⁹ Considering high basicity and tunability of N-aryl guanidines and their propensity to undergo cycloplatination with *cis*-[PtX₂(S(O)Me₂)₂] (X = Cl and TFA) under mild reaction condition, we began a systematic investigation aimed at understanding the structural and photophysical properties of heteroleptic platinacycles, [Pt(TAG)(acac)] (TAG = triarylguanidinate(1⁻)- κ C, κ N; **10-18**) and [Pt(TAG)(pic)] (**19**). The new complexes were fully characterized. DFT and TD-DFT calculations were carried out on **11**, **15**, **18** and **19** to understand the origin of electronic absorption and emission bands.

Results and discussion

Syntheses

Cycloplatinated guanidinate(1⁻) complexes **1-5** were prepared following the literature procedures (see Fig. 2).³⁰⁻³²

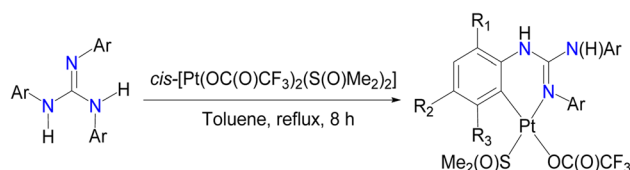
Cycloplatination reactions of *sym* N,N',N''-triarylguanidines, (ArNH)₂C=NAr (*sym* = symmetrical; Ar = 2-XC₆H₄ (X = F, Cl and Br) and 4-FC₆H₄) with *cis*-[Pt(TFA)₂(S(O)Me₂)₂] (TFA = OC(O)CF₃) in toluene under reflux condition for 8 h following the procedure established for **1-5** in our laboratories afforded **6-9** in 75-82% yields as outlined in Scheme 1. Reactions of **1-9** with one equiv. of acetylacetonate (acacH) in the presence of one equiv. of K₂CO₃ in MeCN at 75 °C for 36 h afforded **10**, **11**, **15** and **16** as green crystals and **12-14**, **17** and **18** as yellow crystals



Complex	Ar	R ₁	R ₂	R ₃	X
1	2-(MeO)C ₆ H ₄	OMe	H	H	Cl ^a
2	2-MeC ₆ H ₄	Me	H	H	OC(O)CF ₃ ^b
3	4-MeC ₆ H ₄	H	Me	H	OC(O)CF ₃ ^b
4	2,4-Me ₂ C ₆ H ₃	Me	Me	H	OC(O)CF ₃ ^b
5	2,5-Me ₂ C ₆ H ₃	Me	H	Me	OC(O)CF ₃ ^c

^aRef. 30; ^bRef. 31; ^cRef. 32

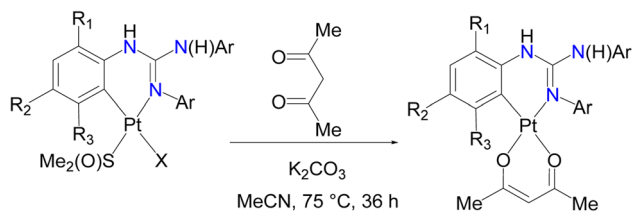
Fig. 2 Known cycloplatinated guanidinate(1⁻) complexes, **1-5**.



Complex	Ar	R ₁	R ₂	R ₃
6	2-FC ₆ H ₄	F	H	H
7	2-ClC ₆ H ₄	Cl	H	H
8	2-BrC ₆ H ₄	Br	H	H
9	4-FC ₆ H ₄	H	F	H

Scheme 1 Syntheses of cycloplatinated guanidinate(1⁻) complexes, **6-9**.





	Ar	R ₁	R ₂	R ₃	
1	2-(MeO)C ₆ H ₄	OMe	H	H	10
2	2-MeC ₆ H ₄	Me	H	H	11
3	4-MeC ₆ H ₄	H	Me	H	12
4	2,4-Me ₂ C ₆ H ₃	Me	Me	H	13
5	2,5-Me ₂ C ₆ H ₃	Me	H	Me	14
6	2-FC ₆ H ₄	F	H	H	15
7	2-ClC ₆ H ₄	Cl	H	H	16
8	2-BrC ₆ H ₄	Br	H	H	17
9	4-FC ₆ H ₄	H	F	H	18
20	C ₆ H ₅	H	H	H	22

X = Cl (**1**) and OC(O)CF₃ (**2–9**).

Scheme 2 Syntheses of heteroleptic cycloplatinated guanidinate(1[−]) complexes, **10–18** and **22**.

in 81–94% yields after work up and crystallization events (see Scheme 2).

Cycloplatination of nitrogen donor ligands can be carried out by thermal method with various Pt(II) sources such as K₂PtCl₄, (Bu₄N)₂PtCl₄ and *cis*-[PtCl₂(S(O)Me₂)₂]. However, this method is plagued with issues such as decomposition of the Pt(II) source to Pt(0) and requires a longer reaction period up to a week thereby producing platinacycles in low to moderate yields. Further, platinacycles of the type **A** have been isolated using more expensive and air-sensitive [PtMe₂(μ-SMe₂)₂] as the Pt(II) precursor.³³ Recently, Gonzalez-Herrero and co-workers reported photochemical pathway for [Bu₄N][Pt(ND)Cl₂] (ND = mono-anionic 2-aryl pyridines-κC,κN and related C,N ligands) from [Bu₄N]₂[Pt₂Cl₆] and the corresponding nitrogen donor ligands. The reaction of [Bu₄N][Pt(ND)Cl₂] even with Na(acac) afforded platinacycles of the type **A** only in 31–65% yields.³⁴ Thus,

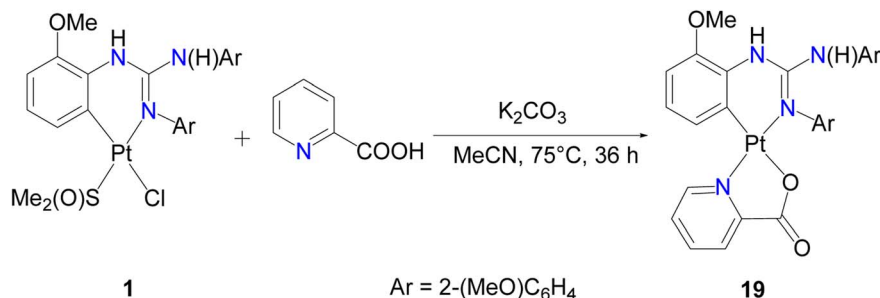
synthetic route outlined in Scheme 2 is operationally simple but yet this route gave the products in good to very good yields.

We have also employed picolinic acid (picH) in place of acacH in the reaction with **1** in order to understand the ring size effect and higher ligand field strength of the picolinate(1[−]) ligand^{1h} on the photophysical properties of the resulting platinacycle, **19**. Thus, **1** was treated with picH under the condition identical to that described in Scheme 2, which enabled us to isolate **19** as green crystals in 89% yield as illustrated in Scheme 3. The reaction involving **20** and acacH in 1 : 1 molar ratio in the presence of K₂CO₃ under the optimised conditions always gave a known dinuclear platinacycle **21**³⁵ instead of the anticipated mononuclear platinacycle, **22** (see Schemes 2 and S1 in the, ESI†).

Solution studies

¹⁹⁵Pt NMR spectroscopy is an important tool to shed light on the coordination environment around the Pt atom in organo-platinum complexes.^{30–32,35–39} Platinacycles of the type **A** have been sparsely characterized by ¹⁹⁵Pt NMR spectroscopy with a few exceptions,^{6,40,41} possibly due to their poor solubility in commonly used NMR solvent, CDCl₃. Platinacycle, **6** was not sufficiently soluble in CDCl₃ for ¹⁹⁵Pt and ¹³C{¹H} NMR measurements. ¹⁹⁵Pt NMR spectra of precursors **7–9** revealed a singlet at δ_{Pt} −3606, −3591 and −3622, respectively. The aforementioned δ_{Pt} values are somewhat comparable with those shifts reported for **1–5** (δ_{Pt} −3737 (**1**),³⁰ −3650 (**2**), −3674 (**3**), −3655 (**4**)³¹ and −3717 (**5**)³²).

Platinacycles **10–18** revealed a single peak in the interval of −2385 to −2527 ppm as listed in Table 1. These δ_{Pt} values of **10–18** are deshielded relative to their precursors **1–9** as reflected from the positive coordination chemical shift, Δδ. This trend either resembles⁴⁰ or opposes⁴¹ the trend reported for five-membered cycloplatinated nitrogen-donor complexes, [Pt(ND)(acac)] and their precursors depending upon the steric/electronic properties of the C,N chelate rings. The downfield δ_{Pt} values of **10–18** is ascribed to the Pt(II) → acac(1[−]) charge transfer process as reported for the related complexes known in the literature.^{6,39a,40,41} Platinacycle **19** revealed a singlet at δ_{Pt} −2906 with a smaller Δδ value of 831 ppm than that of **10** (Δδ = 1312 ppm), which is likely ascribed to the difference in the ring size and the difference in the donor atoms associated with the ancillary ligands.^{36,42}



Scheme 3 Synthesis of cycloplatinated guanidinate(1[−]) complex, **19**.



Table 1 δ_{Pt} (CDCl_3 , 85.8 MHz) and $\Delta\delta$ ($=\delta_{\text{Pt}}[\text{Pt}(\text{TAG})(\text{acac})] - \delta_{\text{Pt}}[\text{Pt}(\text{TAG})\text{X}(\text{S}(\text{O})\text{Me}_2)]$; X = Cl and TFA) values for **10–18** and $\Delta\delta$ ($=\delta_{\text{Pt}}[\text{Pt}(\text{TAG})(\text{pic})] - \delta_{\text{Pt}}[\text{Pt}(\text{TAG})\text{Cl}(\text{S}(\text{O})\text{Me}_2)]$) value for **19**

Complex	δ_{Pt}	$\Delta\delta$	Complex	δ_{Pt}	$\Delta\delta$
10	−2425	1312	15	−2420	− ^a
11	−2425	1225	16	−2393	1213
12	−2451	1223	17	−2385	1206
13	−2438	1217	18	−2423	1199
14	−2527	1190	19	−2906	831

^a δ_{Pt} is not available for the precursor due to its poor solubility in CDCl_3 .

The δ_{Pt} value observed for platinacycles are influenced by both steric and electronic factors.^{30,31,43} The δ_{Pt} value of platinacycles which are ligated with more basic guanidinate(1−) ligand is more shielded than those platinacycles which are ligated with a less basic guanidinate(1−) ligand as can be seen from the shifts of the **11/15** and **12/18** pairs. The more shielded δ_{Pt} value of **12** than that of **11**, as is also observed between **2** and

3, can be ascribed to the difference in the electronic/steric factors associated with the *C,N* chelates. This trend is in line with the trend reported for the known Pt(II) complexes.^{30,31,39b} Complex **14** revealed a smaller $\Delta\delta = 1190$ than **13** ($\Delta\delta = 1217$) which is likely due to greater rigidity of the six-membered [Pt(TAG)] ring in the former complex due to the presence of Me group on the carbon which, is present adjacent to the Pt–C bond. The δ_{Pt} shifts toward downfield upon going from **15** → **16** → **17** and this trend could be ascribed to the difference in both the steric and electronic factors associated with the *C,N* chelate rings.

The δ_{Pt} values reported for **10–18** compare favourably well with that reported for the six-membered cycloplatinated 1,2-diarylimidazolate(1−) complex, [Pt(ND)(acac)] (−2522 ppm).²⁵ The δ_{Pt} value reported for five-membered platinacycles, [Pt(ND)(acac)] varied from −2700 to −2800 ppm,^{6,40,41} more shielded than those shifts reported for **10–18** listed in Table 1. This shift difference could arise due to a combination of electronic, steric factors associated with the *C,N* chelate rings and the difference in the ring size of the [Pt(ND)] units in these two types of platinacycles.⁴²

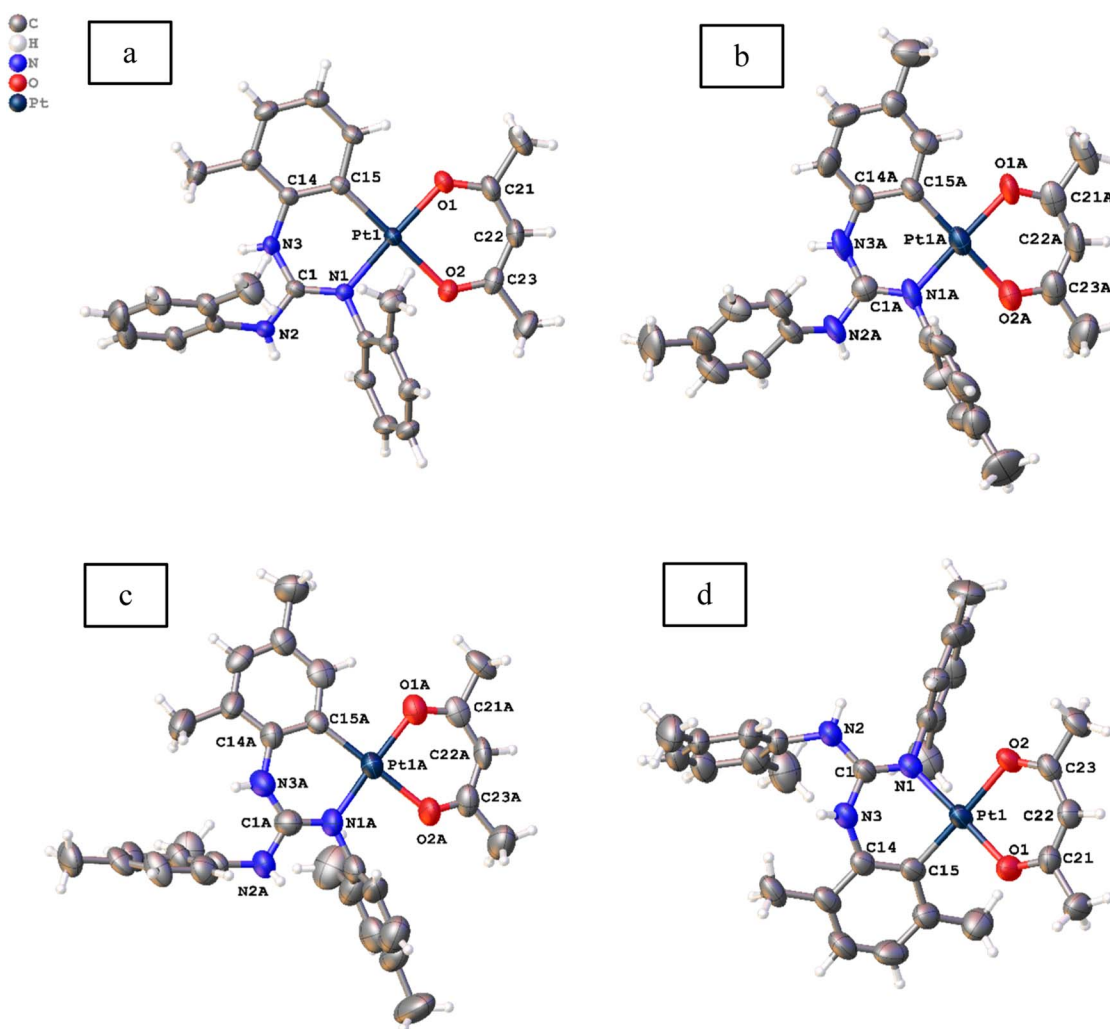


Fig. 3 Molecular structures of **11** (a), **12** ((b) $Z' = 2$), **13** · 0.5 toluene ((c) $Z' = 2$) and **14** (d) at the 50% probability level. Solvent molecule is omitted from **13** · 0.5 toluene for clarity.



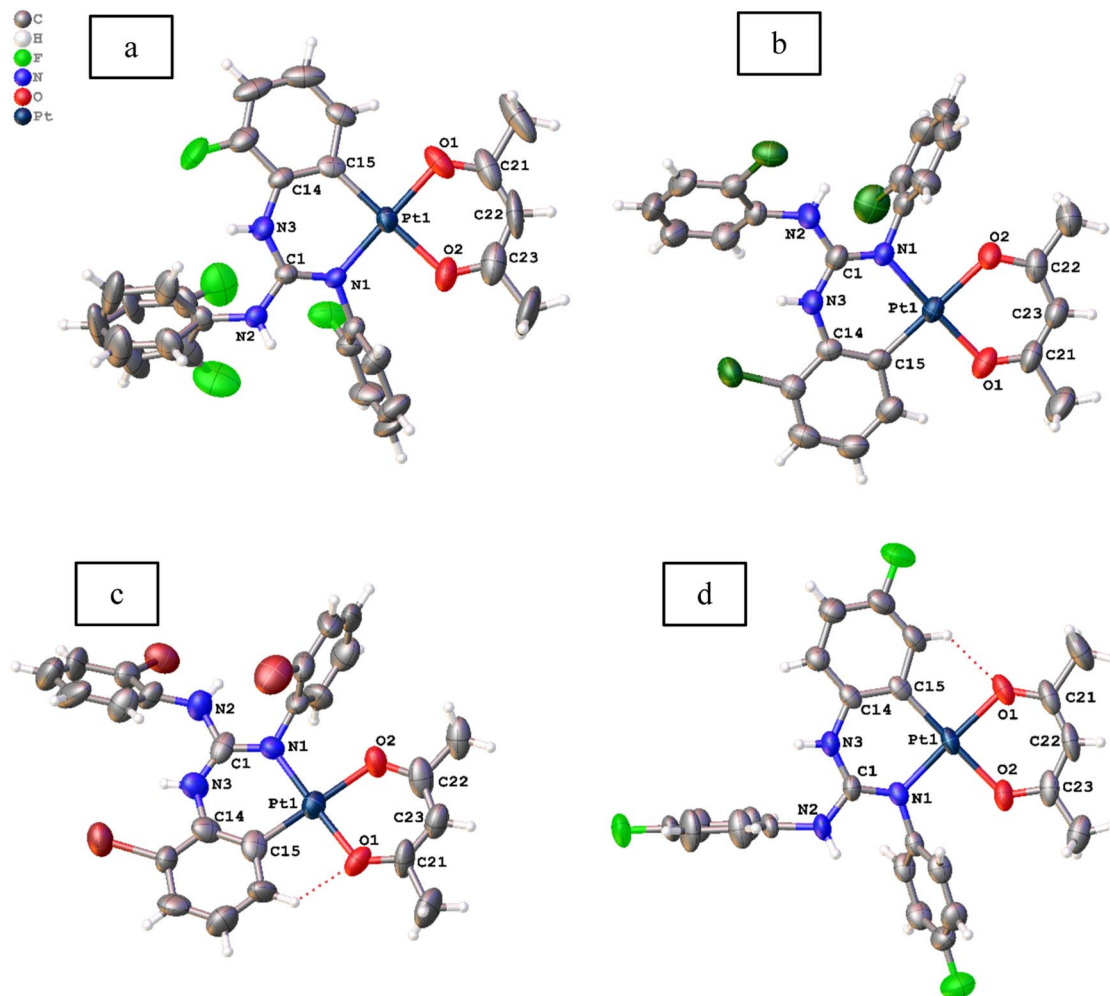


Fig. 4 Molecular structures of 15 (a), 16 (b), 17 (c) and 18 (d) at the 50% probability level.

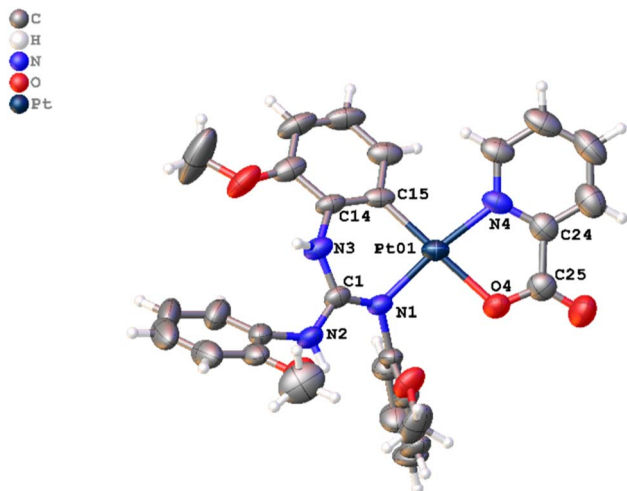


Fig. 5 Molecular structure of 19 at the 50% probability level.

Platinacycles **10–18** contain two types CH_3 protons in the acac(1 $-$) ligand and three types of OCH_3 (**10**)/ CH_3 protons (**11** and **12**) or six types of CH_3 protons (**13** and **14**) in the

guanidinate(1 $-$) ligands. 1H NMR spectroscopy was used to estimate the ratio of CH_3 protons of the acac(1 $-$) ligand to the OCH_3/CH_3 protons present in the guanidinate(1 $-$) ligands. The estimated ratios of about 6 : 9 (**10–12**) or 6 : 18 (**13** and **14**) matched with the anticipated ratios thereby confirming retention of the solid state structures of these platinacycles in solution as well. The ratio of CH_3 protons of the acac(1 $-$) ligand to the aryl protons of the guanidinate(1 $-$) ligands was estimated and the ratios in **10–12** and **13–14** were found to be about 6 : 11 and 6 : 8 ratios, respectively as anticipated for the solid state structures. The presence of a chelating acac(1 $-$) ligand in **10–18** was also inferred from a signature signal assignable to the CH proton at about 5.20 ppm. Platinacycle **18** revealed the presence of two species in solution in about 1.00 : 0.07 ratio as revealed by 1H NMR spectroscopy and the presence of two solution species was independently confirmed by ^{19}F NMR spectroscopy. We believe that these two species arise due to the restricted rotation of the exocyclic (N $_2$)C–N(H)Ar single bond in the six-membered [Pt(TAG)] ring.^{32,37}

The 1H NMR spectrum of **19** revealed three singlets at δ_H 3.80, 3.82 and 4.02 assignable to OCH_3 protons of the



guanidinate(1[−]) ligand and the estimated ratio of these protons to the sum of the aryl protons of the guanidinate(1[−]) and pic(1[−]) ligands was found to be 9:15 thereby confirming retention of the solid structure in solution as well. The ¹³C{¹H} NMR spectral pattern of **10–19** complements their respective ¹H NMR spectral pattern and as anticipated, conforming to their respective solid-state structures.

Molecular and crystal structures

Molecular structures of **11**, **12**, **13**·0.5 toluene and **14–19** were determined by single crystal X-ray diffraction (SCXRD) and are illustrated in Fig. 3–5. The bond parameters around the Pt(II) atom in the above-mentioned complexes are listed in Tables S3–S8 in the ESI.† The Pt(II) atom in all platinumacycles except **19** is simultaneously bonded to the guanidinate(1[−]) and acac(1[−]) ligands in a chelating fashion and simultaneously becomes part of two six-membered [Pt(TAG)] and [Pt(acac)] rings. The key structural parameters of the aforementioned platinumacycles are listed in Table 2. The six-membered [Pt(TAG)] ring revealed a shallow boat (**11**, **12** and **13**·0.5 toluene), sofa (**14**) or deep boat (**19**) conformations. The distinct conformation of the six-membered [Pt(TAG)] ring in **14** arises due to the presence of Me substituent on the aryl carbon which present adjacent to the Pt–C bond while that in **19** arises due to the fact that the Pt(II) atom is also part of the five-membered [Pt(pic)] ring.

Table 2 Key structural parameters of complexes **11**, **12**, **13**·0.5 toluene and **14–18**

	θ_1^a (deg)	θ_2^b (deg)	θ_3^c (deg)	θ_4^d (deg)	θ_5^e (deg)
11	13.2(7)	19.9(3)	5.7(3)	2.7(6)	1.9(2)
12					
Molecule 1	15.3(1)	19.3(1)	1.4(1)	1.2(1)	2.9(3)
Molecule 2	16.0(1)	25.0(1)	2.5(1)	1.1(1)	1.7(3)
13 ·0.5 toluene					
Molecule 1	5.55(6)	12.59(9)	3.10(3)	10.99(9)	2.78(9)
Molecule 2	10.68(4)	9.60(7)	0.66(3)	2.38(4)	2.58(9)
14	34.8(2)	28.4(7)	4.6(3)	2.6(5)	0.4(1.1)
15	12.1(7)	10.5(1)	0.7(7)	3.3(9)	1.9(3)
16	5.3(5)	9.1(8)	0.4(4)	0.7(5)	1.6(3)
17	11.7(2)	4.6(9)	1.8(8)	1.6(1)	2.4(3)
18	4.1(3)	1.1(7)	2.5(3)	12.8(4)	4.3(1)

^a θ_1 is the angle between the mean plane defined by the N1PtC15 and C1N1C14C15 planes. ^b θ_2 is the angle between the mean plane defined by the C1N3C14 and C1N1C14C15 planes. ^c θ_3 is the angle between the mean plane defined by the N1PtC15 and O1Pt1O2 planes. ^d θ_4 is the angle between the mean plane defined by the O1Pt1O2 and O1C21O2C23 planes. ^e θ_5 is the angle between the mean plane defined by the C21C22C23 and O1C21O2C23 planes.

The degree of puckering of the six-membered [Pt(TAG)] and [Pt(acac)] rings and the degree of deviation of the geometry of the Pt(II) atom from the square plane are quantified with θ_1 , θ_2 , θ_3 , θ_4 and θ_5 parameters. The values of $\theta_1 = 15.3(1)^\circ$ (molecule 1) and $16.0(1)^\circ$ (molecule 2) in **12** are higher than the corresponding values observed for **11** ($13.2(7)^\circ$), which possibly arises due to the difference in the packing pattern observed in the solid state. The value of $\theta_1 = 34.8(2)^\circ$ in **14** is significantly greater than the corresponding value observed for **13**·0.5 toluene ($5.55(6)^\circ$ (molecule 1) and $10.68(4)^\circ$ (molecule 2)). The greater value of θ_1 observed for **14** is likely caused by the greater steric hindrance imparted by the Me group on the aryl carbon, which is present adjacent to the Pt–C bond.

The differences in θ_2 value between **11** and **12** (molecule 2) on one hand and **13** and **14** on the other arise due to the difference in the packing pattern of the first pair and variable

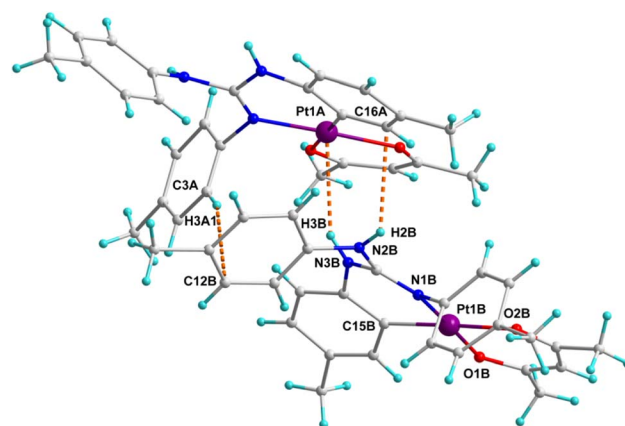


Fig. 6 Packing diagram of **12** ($Z' = 2$) illustrating intermolecular interactions. The intermolecular distances (Å) and angles (deg) are: (i) $N3B \cdots Pt1A = 3.531$, $H3B \cdots Pt1A = 2.767$ and $N3B-H3B \cdots Pt1A = 148.79$. (ii) $C3A \cdots C12B = 3.714$, $H3A1 \cdots C12B = 2.851$ and $C3A-H3A1 \cdots C12B = 154.84$. (iii) $N2B \cdots C16A = 3.086$, $H2B \cdots C16A = 2.823$ and $N2B-H2B \cdots C16A = 119.91$.

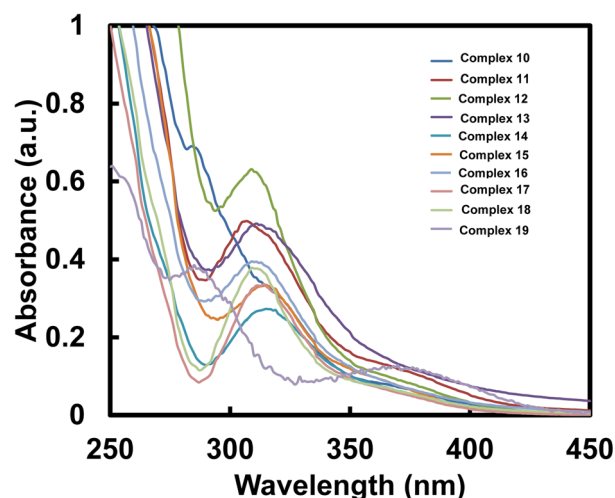


Fig. 7 UV-Visible absorption spectra of **10–19** (10^{-5} M, CH_2Cl_2) measured at RT.



Table 3 Absorption data of 10–19 measured in 10^{-5} M degassed CH_2Cl_2 at RT

Complex	λ_{abs} (nm)	ϵ ($\times 10^4 \text{ M}^{-1} \text{ cm}^{-1}$)	Complex	λ_{abs} (nm)	ϵ ($\times 10^4 \text{ M}^{-1} \text{ cm}^{-1}$)
10	284, 318	6.9, 3.234	15	315	3.346
11	307	4.985	16	309	3.948
12	309	6.315	17	310	3.273
13	311	4.923	18	311	3.766
14	315	2.727	19	285, 370	3.85, 1.28

positions of two Me substituents in the platinated aryl ring in the second pair. The Pt(II) atom deviates from the square plane either slightly (13·0.5 toluene (molecule 2), 15 and 16), moderately (12 (molecules 1 and 2), 13·0.5 toluene (molecule 1), 17 and 18) or significantly (11 and 14) as reflected from value of θ_3 . The extent of folding of Pt1 atom from the basal plane constituted by O1, C21, O2 and C23 atoms in the [Pt(acac)] ring is minimal in 11–18 except in 13·0.5 toluene (molecule 1) and 18 as reflected from the value of θ_4 . The greater folding of acac(1–) ligand along the $\text{O}_1\cdots\text{O}_2$ vector in 13·0.5 toluene (molecule 1) and 18 could arise due to the difference in the intermolecular interactions (see the ESI†). The folding of methine C22 of the acac(1–) ligand from the basal plane constituted by O1, C21, O2, and C23 in all complexes is minimal as reflected from the value of θ_5 . The values of $\theta_1 = 29.6(2)^\circ$, $\theta_2 = 23.6(4)^\circ$ and $\theta_3 = 8.2(1)^\circ$ observed for 19 are greater than the corresponding values observed for 11 as the Pt(II) is part of the five-membered [Pt(pic)] ring in the former complex.

Crystal structures of platinacycles were analysed to understand the nature and types of intermolecular interactions and their possible influence on the shape of the emission bands. Various types intermolecular interactions present in the crystal lattice of 12 are illustrated in Fig. 6 while these interactions in the remaining platinacycles are illustrated in the Fig. S1–S8 in the ESI.† Two molecules were found in an asymmetric unit of 12, and these two molecules are linked through intermolecular $\text{N-H}\cdots\pi$, $\text{C-H}\cdots\pi$ and $\text{N-H}\cdots\text{Pt}$ interactions as illustrated in Fig. 6.

The binding of d^8 metals to the H–X (X = C, N and O) bond through $\text{X-H}\cdots\text{M}$ interaction is being actively studied due to their relevance in the fields of crystal engineering, metal mediated and catalysed X–H bond activation and optical properties.⁴⁴ The bonding in the $\text{X-H}\cdots\text{M}$ unit can be classified as agostic, anagostic and weak hydrogen bonding interactions. An agostic interaction occurs when the $\text{X-H}\cdots\text{M}$ unit is stabilised by 3c–2e bonding with the electron deficient metals, anagostic interaction occurs when the $\text{X-H}\cdots\text{M}$ unit is stabilised by 3c–4e bonding with the electron rich metals. The $\text{N-H}\cdots\text{Pt}$ interaction found in 12 is considered as a weak hydrogen bonding interaction as it fulfils four essential criteria set out by Brammer and co-workers for the $\text{N-H}\cdots\text{Pt}$ hydrogen bonding.⁴⁵ Moreover, the $\text{H3B}\cdots\text{Pt1A} = 2.767$ Å distance and $\text{N3B-H3B}\cdots\text{Pt1A} = 148.79^\circ$ angle found in 12 clearly matched with the corresponding values of 2.1–2.8 Å and 140 – 170° respectively anticipated for the $\text{N-H}\cdots\text{Pt}$ hydrogen bonding interaction reported in the literature.^{45–48} This hydrogen bond is believed to influence both the shape and position of the band in the photoluminescence spectrum of 12 (see later).

Photophysical properties

Electronic absorption spectroscopy. UV-Visible spectra of 10–19 were measured in degassed CH_2Cl_2 and are illustrated in Fig. 7. The values of λ_{max} (nm) and ϵ ($\times 10^4 \text{ M}^{-1} \text{ cm}^{-1}$) are listed in Table 3. Complexes 11, 15, 18 and 19 revealed a band at 307, 315, 311 and 370 nm, which is caused by electronic transition from HOMO–1 to LUMO (11, 15 and 18) or from HOMO to LUMO (19). In addition, complex 19 also revealed one band at 285 nm, which is assigned to HOMO–1 to LUMO transition (see below). Complexes 10, 12, 13, 14, 16 and 17 revealed a band at 318, 309, 311, 315, 309 and 310 nm, respectively. These bands are assigned to HOMO–1 to LUMO electronic transition as analogously invoked for 11, 15 and 18.

Emission studies of crystalline solids. Platinacycles 10–19 were subjected to photoluminescence studies at room

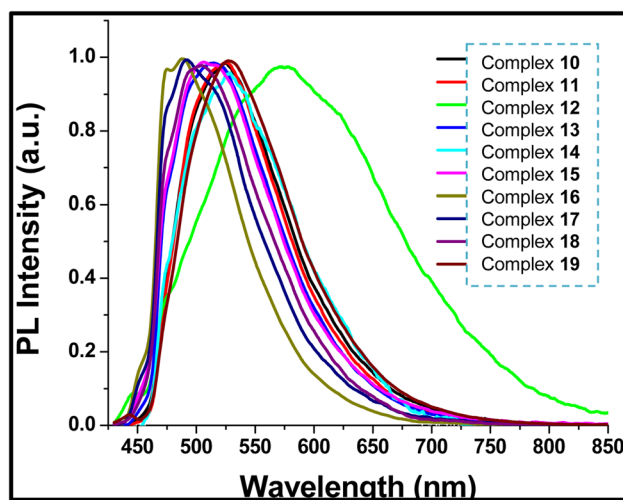


Fig. 8 Normalized room temperature photoluminescence spectra of crystalline samples of 10–19 (excited by 405 nm CW diode laser).

Table 4 Emission data of 10–19 in crystalline form

Complex	λ_{PL}^a (nm)	τ^a (ns)	Complex	λ_{PL}^a (nm)	τ^a (ns)
10	525	1.55	15	506	1.61
11	527	1.79	16	488	1.76
12	570	1.26	17	492	1.53
13	515	1.81	18	503	1.71
14	526	1.68	19	529	1.77

^a ($\lambda_{\text{exc}} = 405$ nm, $\lambda_{\text{em}} = 520$ nm (except for 12, $\lambda_{\text{em}} = 580$ nm)).



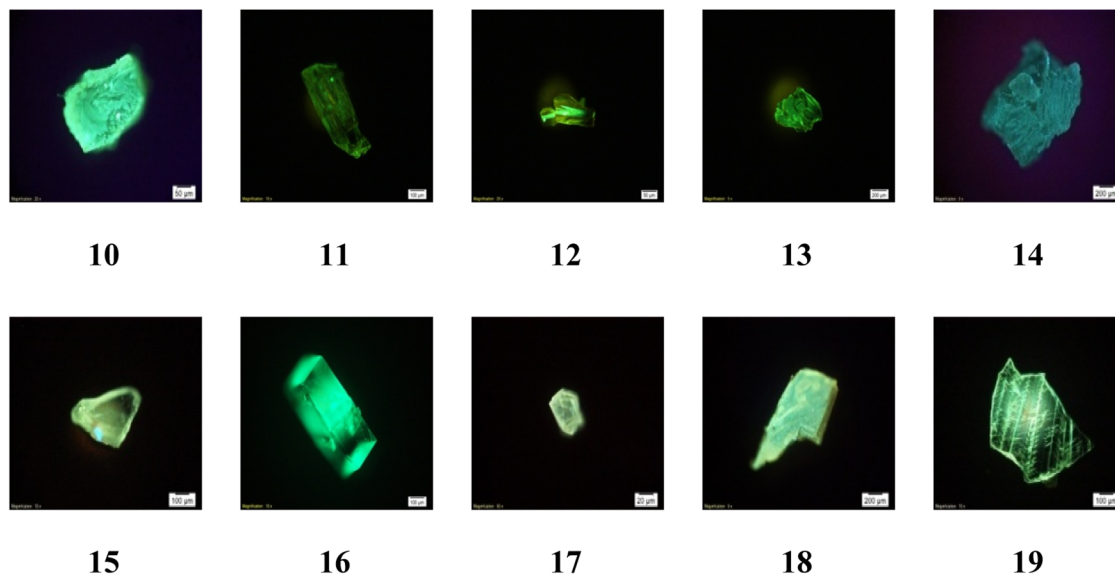


Fig. 9 Photoluminescence microscope images of 10–19 in crystalline form excited by 405 nm CW diode laser.

temperature by exciting the respective single crystals with a low power 405 nm laser excitation source. The results revealed that all the platinacycles displayed emission in blue to green region with λ_{PL} ranging from 488 nm to 570 nm in the visible region. The photoluminescence spectra of 10–19 are shown in Fig. 8 and the respective λ_{PL} values are listed in Table 4. The corresponding photoluminescence images are shown in Fig. 9.

The photoluminescence spectrum of 12 is broader and red shifted than the rest of the platinacycles ($\lambda_{\text{PL}} = 570$ nm (12) and 488–529 nm (10, 11 and 13–19)). In a family of *N*-heterocyclic carbene derived heteroleptic platinacycles of the type C, one complex used to show a broad emission band, which exhibited red shift from the rest of the complexes.^{49,50} However, the reason(s) for the above-mentioned spectral behaviour was not addressed clearly. The broad and red shifted emission band of 12 are ascribed to the presence of an intermolecular N–H⋯Pt, N–H⋯ π and C–H⋯ π interactions between two crystallographically distinct molecules in an asymmetric unit ($Z' = 2$) found in the crystal lattice. The red shift observed for 12 is likely ascribed to destabilisation of the HOMO level, decreasing the luminescence energy.⁵¹ The broadening of photoluminescence spectrum of 12 is likely ascribed to the distortion in the excited state.⁵²

The presence of fluoro substituent in the aryl rings of the guanidinate(1–) ligand in 15 and 18 causes a blue shift of 21 nm and 67 nm, respectively when compared with analogous complexes 11 and 12. Complexes 16 and 17 are also blue shifted by 39 nm and 35 nm respectively when compared to 11. It is to be noted that λ_{PL} observed for 19 closely matches with that observed for 10 suggesting the absence of any significant effect of ancillary ligands pic(1–) and acac(1–) respectively in these complexes, upon the λ_{PL} .

Photoluminescence lifetime studies. The analyses of emission decay curves provide the lifetime of the corresponding excited state species of the platinacycles. The

photoluminescence decay curves for platinacycles 10–19 are illustrated in Fig. 10, which revealed a typical single exponential decay determined by the following equation:

$$I(t) \propto \exp(-t/\tau_{\text{exp}})$$

where $I(t)$ = intensity (*y*-axis), t = time interval (*x*-axis) and τ_{exp} = excited state lifetime.

Emission stability of complex 11. To reveal the emission stability of the platinacycles 10–19, which is an important parameter considered while designing materials for use in light

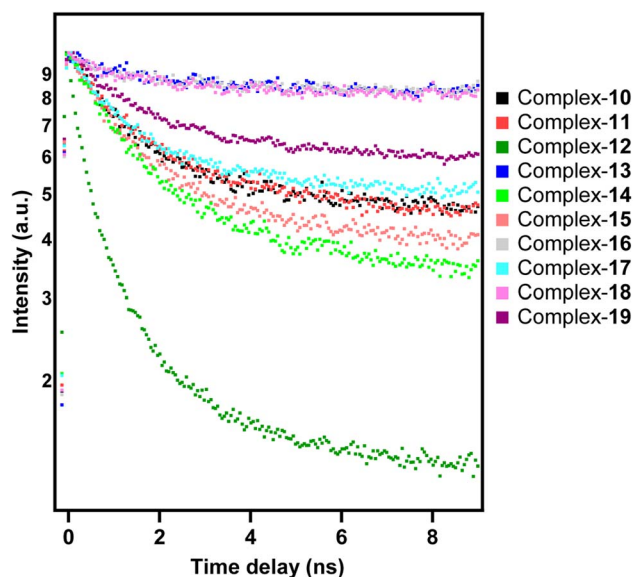


Fig. 10 Time correlated single photon counting (TCSPC) decay curves of 10–19 in crystalline form, monitored at respective emission peak maxima (excited by Ti-sapphire femtosecond laser: 400 nm, 120 fs, 80 MHz).



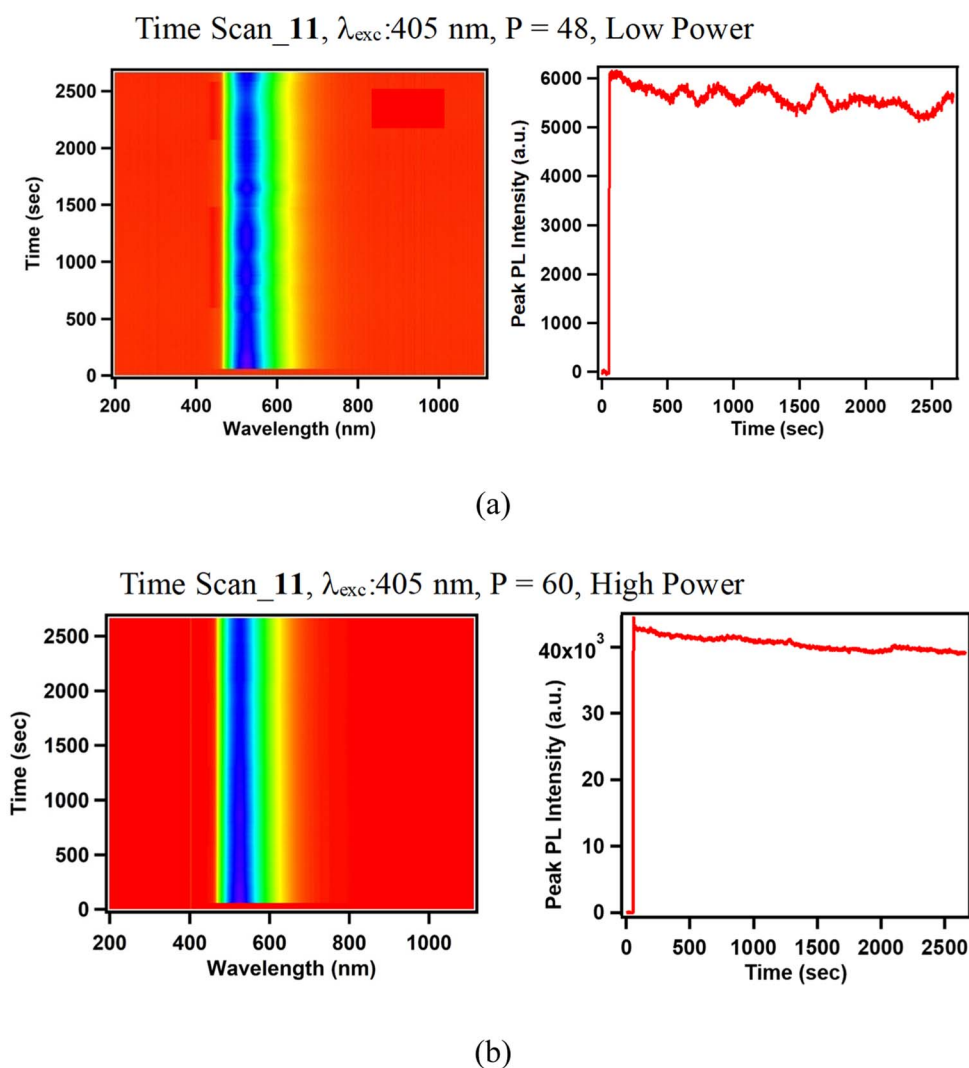


Fig. 11 Photoluminescence stability (time-spectral intensity maps and PL peak maxima time variation) of platinumacycle **11** at (a) low power and (b) high power, excited by 405 nm CW diode laser.

emitting applications, the PL emission profile of platinumacycle **11** was monitored with a 405 nm laser irradiation over a span of more than 40 min under low power ($P = 48$ mW) and high power ($P = 60$ mW) conditions. The results of these experiments are shown in Fig. 11, which clearly indicate that the emission band exhibited by platinumacycle **11** is appreciably stable and revealed no change in the emission spectral pattern under both the conditions of low and high-power laser irradiation even after 40 min. Thus, the new complexes reported herein fulfils several criteria that are essential for OLED emitters.⁵³

DFT and TD-DFT studies

Computational details. The fully optimized geometries of complexes **11**, **15**, **18** and **19** obtained using the density functional theory (B3LYP),^{54–56} selected bond parameters and total energies in ground state are included in the ESI.† F, O, N, C and H atoms were described using the 6-31G* basis set⁵⁷ and the Pt atom was described using the pseudopotential LANL2DZ basis

set.^{58–61} The frequency calculations were also carried out at the B3LYP/6-31G*/LANL2DZ level of theory. All optimized geometries were found to be true minima without any imaginary frequencies. The solvent correction for CH_2Cl_2 was carried out using the polarizable continuum model.^{62–64} The computational analyses were carried out using the Gaussian 09 software.⁶⁵

The TD-DFT calculations were carried out for 12 excited states and the vertical excitation energies (nm) are computed along with their oscillator strength, f . The TD-DFT results for the absorption study in CH_2Cl_2 agree well with that of the experimental data. Maximum absorption is centred around 300 nm for complexes **11**, **15** and **18** and for **19**, additional bands ranging from 350–400 nm are obtained. The frontier molecular orbitals (FMOs) and their calculated energy levels for complexes **11**, **15**, **18** and **19** are illustrated in Fig. 12. For **11**, **15** and **18**, the highest probable transition centered on 300 nm arises due to the singlet transition from HOMO–1 \rightarrow LUMO level ($f > 0.1$). The HOMO–1 of these complexes is located on the

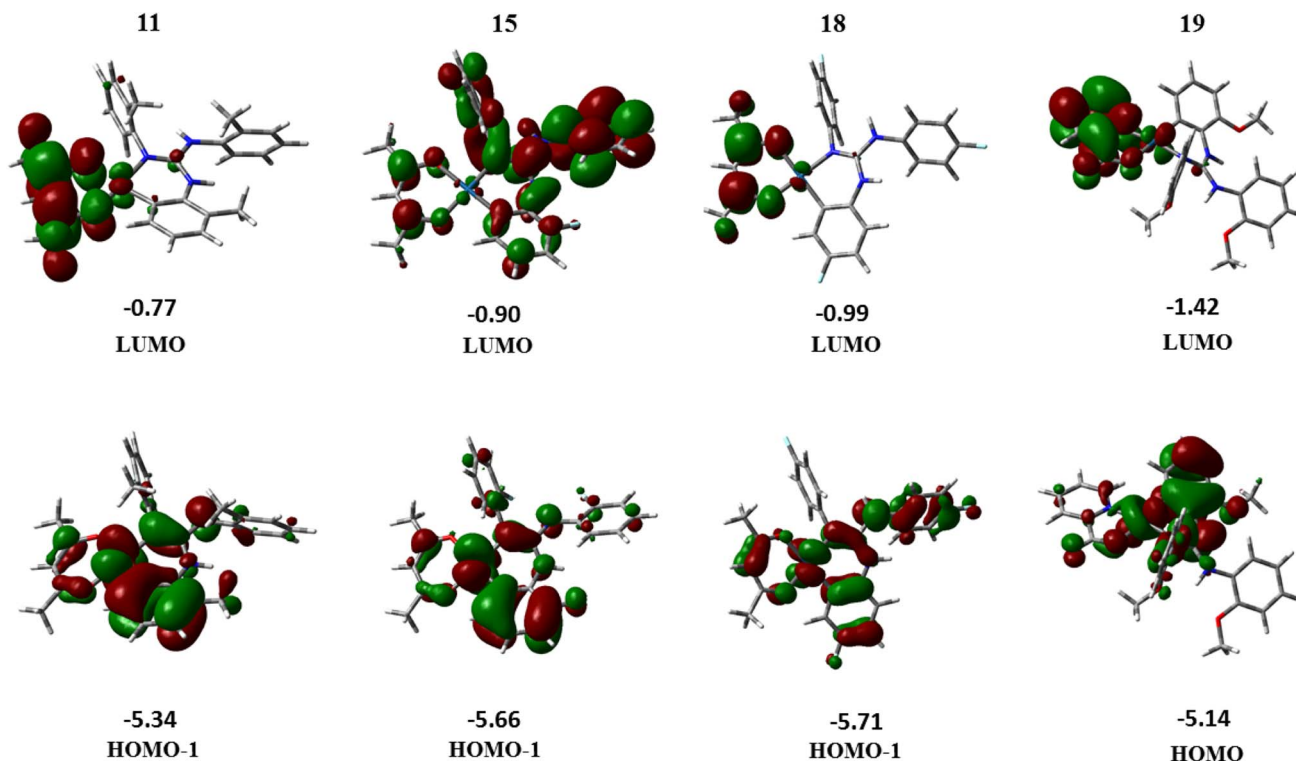


Fig. 12 Molecular orbital diagrams and their calculated energy levels (in eV) for complexes **11**, **15**, **18** and **19**.

Pt-primary ligand (containing the *C,N* donor atoms), whereas the LUMO is located mainly on the acac(1[−]) ligand. Thus, HOMO-1 → LUMO transition can be interpreted as a mixture of MLCT (Pt to the π orbital of primary ligand) and LLCT from the primary ligand to the acac(1[−]) ligand. For complex **19**, the most probable transition is centred on 395 nm and it arises due to the HOMO → LUMO transition ($f = 0.0721$). The simulated UV-Visible profiles of complexes **11**, **15** and **18** and **19** are compiled in the ESI[†] while their corresponding transitions are listed in Table S11.[†] Similarly, the corresponding LUMO → HOMO-1 transition from the singlet excited state to the ground state occurs in **11**, **15** and **18** while complex **19** shows emission from LUMO → HOMO level (see Table S12[†]).

On comparing the experimental and theoretical emission spectra, only the computed spectra of **19** showed most probable emission (LUMO → HOMO, 96%) at 525 nm which is closer to the experimental value ($\lambda_{\text{PL}} = 529$ nm). However, the computed emission spectra of **11**, **15** and **18** showed the most probable emission around 400 nm. These values are different from those experimentally observed λ_{PL} (527 nm (**11**), 506 nm (**15**) and 503 nm (**18**)) for single crystals. The theoretical λ_{PL} values obtained at the B3LYP/6-31G*/LANL2DZ level of theory deviate considerably from those of the experimental results. However, in the emission spectra of **11**, **15** and **18** computed theoretically, a low intensity transition is observed around 500 nm, which occurs due to LUMO → HOMO transition of the complexes involved. This deviation may be rectified perhaps by the use of higher basis set, but due to computational limitations we present the results obtained by the use of the above mentioned level of theory.

Conclusions

In conclusion, we have isolated ten heteroleptic cycloplatinated guanidinate(1[−]) complexes in good to very good yields. The new complexes were characterized by analytical and IR and multinuclear NMR spectroscopic techniques. Molecular and crystal structures of nine complexes were determined by SCXRD. ¹⁹⁵Pt {¹H} NMR spectroscopy of new complexes prepared in this investigation enabled us to unravel the factors such as steric and electronic factors, ring size and nature of donor atom on the observed δ_{Pt} shifts. The variation of steric property of the aryl substituents in the guanidinate(1[−]) ligands influenced the extent of puckering of the six-membered [Pt(TAG)] ring in the structurally characterized complexes more than the geometry of the Pt(II) atom.

A detailed crystal structure analyses carried out on **12** suggest the significance of intermolecular N-H... π , C-H... π and N-H...Pt hydrogen bonding interactions on the anomalous emission spectrum of this complex in the crystalline form. The new complexes were shown to be a green to blue light emitting materials in the solid state. The tunability of aryl substituents in the six-membered [Pt(TAG)] ring affected the emission properties of certain complexes to some extent while the ancillary ligand affected the emission to a lesser extent (**10** versus **19**). The FMOs involved in the absorption and emission of **11**, **15** and **18** were shown to be HOMO-1 and LUMO while the FMOs of **19** were shown to be HOMO and LUMO. By a judicious combination of the primary and ancillary ligands in the new platina-cycles, better materials for the purpose of OLED fabrication can be further developed.



Experimental section

Platinacycle 6

Cis-[Pt(TFA)₂(S(O)Me₂)₂] (50.0 mg, 0.09 mmol) and the guanidine (ArNH)₂C=NAr (Ar = 2-FC₆H₄; 34.2 mg, 0.09 mmol) were taken in a 25 mL RB flask and dispersed in toluene (10 mL). The RB flask was fitted with a double surface condenser capped with a freshly prepared anhydrous CaCl₂ guard tube. The reaction mixture was refluxed for 8 h, cooled and filtered. The volume of the filtrate was reduced to about 3 mL and stored at RT for two days to afford **6** as colourless crystals. Yield = 75% (47.4 mg, 0.065 mmol). Mp: 240.2 °C. ATR-IR (cm⁻¹): ν(NH) 3306 (m); ν_a(OCO) 1688 (s); ν(C=N) 1622 (m); ν_s(OCO) 1344 (m); ν(S=O) 1190 (s). Anal. calcd for C₂₃H₁₉N₃O₃F₆Spt (M_w = 726.56 g mol⁻¹): C, 38.02; H, 2.64; N, 5.78; S, 4.41. Found: C, 37.88; H, 2.63; N, 5.83; S, 4.61. ESI mass (HRMS) *m/z* [ion]: calcd 613.0849 [M – TFA]⁺. Found 613.0851. ¹H NMR (CDCl₃, 400 MHz): δ_H 3.19 (br, 6H, (CH₃)₂S(O)), 6.40 (s, 1H, NH), 6.83–6.88, 6.92–6.99 (each m, 2 × 1H, ArH), 7.16–7.23 (m, 4H, ArH), 7.25 (br, 1H, NH), 7.27–7.38 (m, 4H, ArH), 7.72 (d, J_{HH} = 8.4 Hz; 1H, ArH). ¹⁹F{¹H} NMR (CDCl₃, 376.31 MHz): δ_F –74.4, –119.5, –122.7, –133.5 (J_{F–Pt} = 41.4 Hz).

Platinacycle 7

Platinacycle **7** was prepared from *cis*-[Pt(TFA)₂(S(O)Me₂)₂] (50.00 mg, 0.087 mmol) and the guanidine (ArNH)₂C=NAr (Ar = 2-ClC₆H₄; 34.2 mg, 0.087 mmol) in toluene (10 mL) by following the procedure previously mentioned for **6**. Platinacycle **7** was obtained as colourless crystals in 82% (55.3 mg, 0.071 mmol) yield. Mp: 209.8 °C. ATR-IR (cm⁻¹): ν(NH) 3364 (m); ν_a(OCO) 1680 (s); ν(C=N) 1607 (m), 1568; ν_s(OCO) 1356 (m); ν(S=O) 1186 (s). Anal. calcd for C₂₃H₁₉N₃O₃F₃Cl₃Spt (M_w = 775.91): C, 35.60; H, 2.47; N, 5.42; S, 4.13. Found: C, 35.66; H, 2.74; N, 5.68; S, 4.43. ESI mass (HRMS) *m/z* [ion]: calcd 662.0040 [M – TFA + H]⁺. Found 661.9937. ¹H NMR (CDCl₃, 400 MHz): δ_H 3.17 (br, 6H, (CH₃)₂S(O)), 6.39 (s, 1H, NH), 6.88 (t, J_{HH} = 8.0 Hz, 1H, ArH), 7.09 (dd, J_{HH} = 8.0 Hz; 1.2 Hz, 1H, ArH), 7.24–7.28, 7.30–7.33 (each m, 2 × 1H, ArH), 7.34 (s, 1H, NH), 7.37–7.40, 7.48–7.51 (each m, 2 × 3H, ArH), 7.86 (dd, J_{HH} = 8.0 Hz; 1.6 Hz, 1H, ArH). ¹³C{¹H} NMR (CDCl₃, 100.5 MHz): δ_C 45.1, 45.9, 110.5, 117.0 (q, J_{C–F} = 290.9 Hz), 119.9, 124.2 (J_{Pt–C} = 34.7 Hz), 125.6, 128.0, 128.3, 128.7, 128.9, 129.1, 129.6, 131.1, 131.4, 131.7, 132.2, 132.6, 137.4, 139.6, 148.2, 161.7 (q, J_{C–F} = 36.3 Hz). ¹⁹F{¹H} NMR (CDCl₃, 376.31 MHz): δ_F –74.4. ¹⁹⁵Pt{¹H} NMR (CDCl₃, 85.78 MHz): δ_{Pt} –3606.

Platinacycle 8

Platinacycle **8** was prepared from *cis*-[Pt(TFA)₂(S(O)Me₂)₂] (50.00 mg, 0.087 mmol) and the guanidine (ArNH)₂C=NAr (Ar = 2-BrC₆H₄; 46.1 mg, 0.087 mmol) in toluene (10 mL) by following the procedure previously mentioned for **6**. Platinacycle **8** was obtained as colourless crystals in 76% (60.0 mg, 0.066 mmol) yield. Mp: 198.1 °C. ATR-IR (cm⁻¹): ν(NH) 3354 (m); ν_a(OCO) 1686 (s); ν(C=N) 1613 (m); ν_s(OCO) 1360 (m); ν(S=O) 1130 (s). Anal. calcd for C₂₃H₁₉N₃O₃F₃Br₃Spt (M_w = 905.83): C, 30.38; H, 2.11; N, 4.62; S, 3.53. Found: C, 30.04; H, 2.09; N,

4.56; S, 3.91. ESI mass (HRMS) *m/z* [ion]: calcd 795.8504 [M – TFA + H]⁺. Found 795.8481. ¹H NMR (CDCl₃, 400 MHz): δ_H 3.16, 3.20 (each s, 2 × 3H, (CH₃)₂S(O)), 6.32 (s, 1H, NH), 6.79 (t, J_{HH} = 7.8 Hz, 1H, ArH), 7.17–7.24 (m, 4H, ArH), 7.37–7.44 (m, 4H, ArH) (3H), NH (1H)), 7.68, 7.70 (each d, J_{HH} = 3.2 Hz, 2 × 1H, ArH), 7.88 (d, J_{HH} = 8.4 Hz, 1H, ArH). ¹³C{¹H} NMR (CDCl₃, 100.5 MHz): δ_C 44.6, 46.1, 110.1, 110.8, 116.9 (q, J_{C–F} = 292.0 Hz), 122.3, 122.5, 124.6, 128.5, 128.8, 128.9, 129.0, 129.2, 129.5, 130.2, 133.3, 133.5, 134.2, 134.3, 138.0, 141.0, 148.5, 161.6 (q, J_{C–F} = 36.3 Hz). ¹⁹F{¹H} NMR (CDCl₃, 376.31 MHz): δ_F –74.4. ¹⁹⁵Pt{¹H} NMR (CDCl₃, 85.78 MHz): δ_{Pt} –3591.

Platinacycle 9

Platinacycle **9** was prepared from *cis*-[Pt(TFA)₂(S(O)Me₂)₂] (50.0 mg, 0.087 mmol) and the guanidine (ArNH)₂C=NAr (Ar = 4-FC₆H₄; 30.0 mg, 0.087 mmol) in toluene (10 mL) by following the procedure previously mentioned for **6**. Platinacycle **9** was obtained as colourless crystals in 78% (49.4 mg, 0.068 mmol) yield. Mp: 227.7 °C. ATR-IR (cm⁻¹): ν(NH) 3314 (m); ν_a(OCO) 1686 (s); ν(C=N) 1618 (m); ν_s(OCO) 1343 (m); ν(S=O) 1113 (s). Anal. calcd for C₂₃H₁₉N₃O₃F₆Spt (M_w = 726.56): C, 38.02; H, 2.64; N, 5.78; S, 4.41. Found: C, 38.41; H, 3.01; N, 6.17; S, 4.78. ESI mass (HRMS) *m/z* [ion]: calcd: 613.0849 [M – TFA]⁺. Found: 613.0913. ¹H NMR (CDCl₃, 400 MHz): δ_H 3.16 (br, 6H, (CH₃)₂S(O)), 6.39–6.42 (m, 1H, ArH), 6.46 (s, 1H, NH), 6.73 (dt, J_{HH} = 8.0 Hz; 2.8 Hz, 1H, ArH), 7.07–7.22 (m, 9H, ArH (8H), NH (1H)), 7.69 (dd, J_{HH} = 10.6 Hz; 2.6 Hz, 1H, ArH). ¹³C{¹H} NMR (CDCl₃, 100.5 MHz): δ_C 45.42, 111.01 (d, J_{C–F} = 6.8 Hz), 112.11 (d, J_{C–F} = 23.1 Hz), 115.70 (d, J_{C–F} = 8.6 Hz), 116.90 (q, J_{C–F} = 290.5 Hz), 116.91 (d, J_{C–F} = 23.1 Hz), 117.66 (d, J_{C–F} = 23.1 Hz), 124.43 (d, J_{C–F} = 21.2 Hz), 128.45 (d, J_{C–F} = 8.7 Hz), 128.70 (d, J_{C–F} = 7.6 Hz), 131.11, 133.53, 138.35, 149.17, 158.52 (d, J_{C–F} = 244.6 Hz), 160.54 (d, J_{C–F} = 62.6 Hz), 161.75 (q, J_{C–F} = 36.6 Hz), 163.02 (d, J_{C–F} = 65.5 Hz). ¹⁹F{¹H} NMR (CDCl₃, 376.31 MHz): δ_F –74.6, –111.6, –113.8, –118.3. ¹⁹⁵Pt{¹H} NMR (CDCl₃, 85.78 MHz): δ_{Pt} –3622.

Platinacycle 10

Platinacycle **10** (50.0 mg, 0.073 mmol) and acetylacetone (8.7 mg, 0.0087 mmol) were dispersed in a freshly distilled acetonitrile (15 mL) in a 25 mL RB-flask and the flask was fitted with an air condenser. K₂CO₃ (12.1 mg, 0.087 mmol) was added to the reaction mixture, the contents in the flask were simultaneously stirred and heated to 75 °C for 36 h. Subsequently, the reaction mixture was cooled and the volatiles were completely removed under vacuum to afford yellow solid. To the solid, CH₂Cl₂ (10 mL) was added and filtered using a Whatman filter paper. The filtrate was concentrated under vacuum to about 2 mL, layered with toluene (2 mL) and stored at RT for 10 days to afford **10** as green crystals suitable for SCXRD. Yield = 92% (44.9 mg, 0.067 mmol). Mp: 206.0 °C. Anal. calcd for C₂₇H₂₉O₅N₃Pt (M_w = 670.63): C, 48.36; H, 4.36; N, 6.27. Found: C, 48.53; H, 3.95; N, 6.25. ATR-IR (cm⁻¹): ν(N–H) 3382 (m), ν(C=N) 1624 (m), ν(C–O) (acac(1–)) 1572 (s), ν(C–O) (acac(1–)) 1546 (s). ESI mass (HRMS) *m/z* [ion]: calcd: 671.1833 [M + H]⁺. Found: 671.1804. ¹H NMR (CDCl₃, 400 MHz): δ_H 1.36, 1.84 (each s, 2 ×



3H, CH₃, acac(1-)), 3.74, 3.81, 3.95 (each s, 3 × 3H, OCH₃), 5.20 (s, 1H, CH, acac(1-)), 6.59 (dd, *J*_{HH} = 8.0 Hz; 1.2 Hz, 1H, ArH), 6.84 (s, 1H, NH), 6.88–6.96 (m, 5H, ArH), 7.09 (dt, *J*_{HH} = 8.0 Hz; 1.3 Hz, 1H, ArH), 7.18 (dt, *J*_{HH} = 7.8 Hz; 1.6 Hz, 1H, ArH), 7.27 (dd, *J*_{HH} = 8.2 Hz; 1.8 Hz, 1H, ArH), 7.33 (dt, *J*_{HH} = 6.4 Hz; 1.6 Hz, 2H, ArH), 8.05 (s, 1H, NH). ¹³C{¹H} NMR (CDCl₃, 100.5 MHz): δ_C 27.0, 27.1, 55.5, 55.9, 56.2, 101.3, 105.1, 111.1, 111.5, 111.7, 121.0, 121.7, 125.1, 126.3, 127.2, 127.3, 130.2, 133.8, 143.8, 145.0, 150.8, 155.0, 183.2, 184.6.

Platinacycle 11

Platinacycle 11 was prepared from 2 (50.0 mg, 0.070 mmol), acetylacetone (8.4 mg, 0.084 mmol) and K₂CO₃ (11.6 mg, 0.084 mmol) in acetonitrile (15 mL) and purified as described previously for platinacycle 10. The solid obtained after removal of the volatiles from the reaction mixture was dissolved in CH₂Cl₂ (2 mL), layered with toluene (2 mL) and stored at RT for 7 days to afford 11 as bright yellow crystals suitable for SCXRD. Yield = 94% (41.1 mg, 0.066 mmol). Mp: 236.2 °C. Anal. calcd for C₂₇H₂₉O₂N₃Pt (*M*_w = 622.19): C, 52.08; H, 4.69; N, 6.75. Found: C, 52.09; H, 4.69; N, 6.75. ATR-IR (cm⁻¹): ν(N-H) 3404 (m), ν(C=N) 1624 (m), ν(C-O) (acac(1-)) 1574 (s), ν(C-O) (acac(1-)) 1541 (s). ESI mass (HRMS) *m/z* [ion]: calcd: 623.1986 [M + H]⁺. Found: 626.1814. ¹H NMR (CDCl₃, 400 MHz): δ_H 1.35, 1.70 (each s, 2 × 3H, CH₃, acac(1-)), 1.85, 2.19, 2.42 (each s, 3 × 3H, CH₃), 5.22 (s, 1H, CH, acac(1-)), 5.69, 6.54 (each s, 2 × 1H, NH), 6.74 (d, *J*_{HH} = 7.2 Hz, 1H, ArH), 6.81 (t, *J*_{HH} = 7.6 Hz, 1H, ArH), 7.15–7.24 (m, 4H, ArH), 7.27–7.32 (m, 4H, ArH), 7.65 (d, *J*_{HH} = 7.6 Hz, 1H, ArH). ¹³C{¹H} NMR (CDCl₃, 100.5 MHz): δ_C 17.1, 17.9, 18.2, 26.8, 27.1, 101.3, 108.5, 119.3, 120.8, 125.6, 126.7, 126.8, 127.9, 128.2, 128.4, 128.8, 130.6, 131.9, 132.4, 134.5, 135.6, 136.1, 136.3, 142.2, 144.1, 183.3, 184.9.

Platinacycle 12

Platinacycle 12 was prepared from 3 (50.0 mg, 0.070 mmol), acetylacetone (8.4 mg, 0.084 mmol) and K₂CO₃ (11.6 mg, 0.084 mmol) in acetonitrile (15 mL) and purified as described previously for platinacycle 10. The solid obtained after removal of the volatiles from the reaction mixture was dissolved in CH₂Cl₂ (2 mL), layered with toluene (2 mL) and stored at RT for 7 days to afford 12 as yellow crystals suitable for SCXRD. Yield = 89% (38.6 mg, 0.062 mmol). Mp: 166.9 °C. Anal. calcd for C₂₇H₂₉O₂N₃Pt (*M*_w = 622.63): C, 52.08; H, 4.69; N, 6.75. Found: C, 52.35; H, 4.89; N, 6.98. ATR-IR (cm⁻¹): ν(N-H) 3399 (m), ν(C=N) 1624 (m), ν(C-O) (acac(1-)) 1574 (s), ν(C-O) (acac(1-)) 1510 (s). ESI mass (HRMS) *m/z* [ion]: calcd: 623.1986 [M + H]⁺. Found: 623.1956. ¹H NMR (CDCl₃, 400 MHz): δ_H 1.45, 1.87 (each s, 2 × 3H, CH₃, acac(1-)), 2.29 (s, 3H, CH₃), 2.35 (s, 2 × 3H, CH₃), 5.24 (s, 1H, CH, acac(1-)), 5.94 (s, 1H, NH), 6.26 (d, *J*_{HH} = 8.0 Hz, 1H, ArH), 6.50 (s, 1H, NH), 6.73 (d, *J*_{HH} = 8.0 Hz, 1H, ArH), 6.96 (d, *J*_{HH} = 8.0 Hz, 2H, ArH), 7.15–7.20 (m, 6H, ArH), 7.51 (s, 1H, ArH). ¹³C{¹H} NMR (CDCl₃, 100.5 MHz): δ_C 21.0, 21.1, 21.3, 27.1, 27.2, 101.4, 109.6, 112.9, 124.4, 125.3, 128.0, 129.5, 130.6, 130.8, 133.9, 134.0, 134.8, 135.7, 135.9, 137.0, 141.1, 145.4, 183.1, 184.8.

Platinacycle 13

Platinacycle 13 was prepared from 4 (50.0 mg, 0.066 mmol), acetylacetone (7.9 mg, 0.079 mmol) and K₂CO₃ (11.2 mg, 0.079 mmol) in acetonitrile (15 mL) and purified as described previously for platinacycle 10. The solid obtained after removal of the volatiles from the reaction mixture was dissolved in CH₂Cl₂ (2 mL), layered with toluene (2 mL) and stored at RT for 5 days to afford 13·0.5 toluene as yellow crystals suitable for SCXRD. Yield = 83% (36.9 mg, 0.055 mmol). Mp: 152.4 °C. Anal. calcd for C₃₀H₃₅O₂N₃Pt (*M*_w = 664.71): C, 54.21; H, 5.31; N, 6.32. Found: C, 54.45; H, 5.66; N, 6.50. ATR-IR (cm⁻¹): ν(N-H) 3406 (m), ν(C=N) 1620 (m), ν(C-O) (acac(1-)) 1574 (s), ν(C-O) (acac(1-)) 1512 (s). ESI mass (HRMS) *m/z* [ion]: calcd: 665.2455 [M + H]⁺. Found: 665.2456. ¹H NMR (CDCl₃, 400 MHz): δ_H 1.40, 1.69 (each s, 2 × 3H, CH₃, acac(1-)), 1.86, 2.14, 2.24, 2.32, 2.33, 2.36 (each s, 6 × 3H, CH₃), 5.22 (s, 1H, CH, acac(1-)), 5.65, 6.45 (each s, 2 × 1H, NH), 6.55 (s, 1H, ArH), 7.02–7.07 (m, 4H, ArH), 7.10 (s, 1H, ArH), 7.14 (d, *J*_{HH} = 7.6 Hz, 1H, ArH), 7.42 (s, 1H, ArH). ¹³C{¹H} NMR (CDCl₃, 100.5 MHz): δ_C 17.1, 17.9, 18.2, 21.1, 21.2, 27.0, 27.2, 101.2, 108.6, 119.0, 126.6, 127.1, 128.1, 128.3, 128.4, 129.6, 131.2, 131.8, 132.5, 132.8, 133.6, 135.7, 136.0, 136.1, 138.7, 139.6, 144.6, 183.1, 184.8.

Platinacycle 14

Platinacycle 14 was prepared from 5 (50.0 mg, 0.066 mmol), acetylacetone (7.9 mg, 0.079 mmol) and K₂CO₃ (11.2 mg, 0.079 mmol) in acetonitrile (15 mL) and purified as described previously for platinacycle 10. The solid obtained after removal of the volatiles from the reaction mixture was dissolved in CH₂Cl₂ (2 mL), layered with toluene (2 mL) and stored at RT for 9 days to afford 14 as yellow crystals suitable for SCXRD. Yield = 86% (37.8 mg, 0.057 mmol). Mp: 190.4 °C. Anal. calcd for C₃₀H₃₅O₂N₃Pt (*M*_w = 664.71): C, 54.21; H, 5.31; N, 6.32. Found: C, 54.57; H, 5.62; N, 6.27. ATR-IR (cm⁻¹): ν(N-H) 3417 (m), ν(C=N) 1631 (m), ν(C-O) (acac(1-)) 1613 (s), ν(C-O) (acac(1-)) 1582 (s). ESI mass (HRMS) *m/z* [ion]: calcd: 665.2455 [M + H]⁺. Found: 665.2467. ¹H NMR (CDCl₃, 400 MHz): δ_H 1.60, 1.70 (each s, 2 × 3H, CH₃, acac(1-)), 1.71, 2.09, 2.25, 2.29, 2.34, 2.64 (each s, 6 × 3H, CH₃), 5.23 (s, 1H, CH, acac(1-)), 5.81, 6.35 (each s, 2 × 1H, NH), 6.58, 6.68 (each d, *J*_{HH} = 7.2 Hz, 2 × 1H, ArH), 6.91 (s, 1H, ArH), 6.97 (d, *J*_{HH} = 6.8 Hz, 1H, ArH), 7.04 (d, *J*_{HH} = 8.0 Hz, 1H, ArH), 7.14 (t, *J*_{HH} = 7.0 Hz, 2H, ArH), 7.20 (s, 1H, ArH). ¹³C{¹H} NMR (CDCl₃, 100.5 MHz): δ_C 16.6, 17.5, 17.9, 20.8, 21.1, 23.7, 26.2, 27.7, 101.3, 113.1, 117.2, 124.3, 125.5, 127.4, 128.2, 128.9, 129.1, 130.9, 131.6, 132.2, 134.5, 136.0, 137.7, 138.4, 141.6, 144.3, 148.3, 182.0, 184.4.

Platinacycle 15

Platinacycle 15 was prepared from 6 (50.0 mg, 0.069 mmol), acetylacetone (8.3 mg, 0.083 mmol) and K₂CO₃ (11.5 mg, 0.083 mmol) in acetonitrile (15 mL) and purified as described previously for platinacycle 10. The solid obtained after removal of the volatiles from the reaction mixture was dissolved in CH₂Cl₂ (2 mL), layered with toluene (2 mL) and stored at RT for 5 days to afford 15 as green crystals suitable for SCXRD. Yield = 81%



(35.5 mg, 0.056 mmol). Mp: 201.8 °C. Anal. calcd for $C_{24}H_{20}F_3O_2N_3Pt$ ($M_w = 634.52$): C, 45.43; H, 3.18; N, 6.62. Found: C, 45.69; H, 3.09; N, 6.25. ATR-IR (cm^{-1}): $\nu(N-H)$ 3406 (m), $\nu(C=N)$ 1630 (m), $\nu(C-O)$ (acac(1-)) 1581 (s), $\nu(C-O)$ (acac(1-)) 1544 (s). ESI mass (HRMS) m/z [ion]: calcd: 635.1234 $[M + H]^+$. Found: 635.1238. 1H NMR ($CDCl_3$, 400 MHz): δ_H 1.42, 1.88 (each s, $2 \times 3H$, CH_3 , acac(1-)), 5.26 (s, 1H, CH , acac(1-)), 5.93 (s, 1H, NH), 6.72–6.77, 6.89–6.93 (each m, $2 \times 1H$, ArH), 7.14–7.24 (m, 5H, ArH (4H), NH (1H)), 7.27–7.39 (m, 4H, ArH), 7.51 (d, $J_{HH} = 8.0$ Hz, 1H, ArH). $^{13}C\{^1H\}$ NMR ($CDCl_3$, 100.5 MHz): δ_C 26.8, 27.0, 101.6, 109.1 (d, $J_{C-F} = 18.3$ Hz), 112.6, 116.1 (d, $J_{C-F} = 20.2$ Hz), 117.2 (d, $J_{C-F} = 19.3$ Hz), 121.6 (d, $J_{C-F} = 6.7$ Hz), 124.2 (d, $J_{C-F} = 12.5$ Hz), 124.5 (d, $J_{C-F} = 2.9$ Hz), 125.2 (d, $J_{C-F} = 5.7$ Hz), 125.6 (d, $J_{C-F} = 3.8$ Hz), 126.2, 128.5 (d, $J_{C-F} = 7.7$ Hz), 128.7 (d, $J_{C-F} = 7.7$ Hz), 129.0 (d, $J_{C-F} = 1.9$ Hz), 130.3, 130.8 (d, $J_{C-F} = 13.6$ Hz), 143.7, 149.4 (d, $J_{C-F} = 244.7$ Hz), 155.9 (d, $J_{C-F} = 185.8$ Hz), 158.4 (d, $J_{C-F} = 184.9$ Hz), 183.6, 185.2. $^{19}F\{^1H\}$ NMR ($CDCl_3$, 376.31 MHz): δ_F -137.4 ($J_{Pt-F} = 40.3$ Hz), -123.6, -120.6.

Platinacycle 16

Platinacycle 16 was prepared from 7 (50.0 mg, 0.064 mmol), acetylacetone (7.7 mg, 0.077 mmol) and K_2CO_3 (10.6 mg, 0.077 mmol) in acetonitrile (15 mL) and purified as described previously for platinacycle 10. The solid obtained after removal of the volatiles from the reaction mixture was dissolved in CH_2Cl_2 (2 mL), layered with toluene (2 mL) and stored at RT for 5 days to afford 16 as green crystals suitable for SCXRD. Yield = 94% (40.9 mg, 0.060 mmol). Mp: 228.0 °C. Anal. calcd for $C_{24}H_{20}Cl_3O_2N_3Pt$ ($M_w = 683.88$): C, 42.15; H, 2.95; N, 6.14. Found: C, 42.45; H, 2.98; N, 6.21. ATR-IR (cm^{-1}): $\nu(N-H)$ 3368 (m); $\nu(C=N)$ 1628 (m); $\nu(C-O)$ (acac(1-)) 1576 (s); $\nu(C-O)$ (acac(1-)) 1516 (s). ESI mass (HRMS) m/z [ion] calcd: 683.0347 $[M + H]^+$. Found: 683.0416. 1H NMR ($CDCl_3$, 400 MHz): δ_H 1.41, 1.88 (each s, $2 \times 3H$, CH_3 , acac(1-)), 5.26 (s, 1H, CH , acac(1-)), 6.01 (s, 1H, NH), 6.87 (t, $J_{HH} = 7.8$ Hz, 1H, ArH), 7.03 (dd, $J_{HH} = 7.8$ Hz; 1.4 Hz, 1H, ArH), 7.23–7.25 (m, 2H, ArH (1H), NH (1H)), 7.34 (dq, $J_{HH} = 8.0$ Hz; 1.5 Hz, 2H, ArH), 7.40–7.49 (m, 4H, ArH), 7.69–7.72 (m, 2H, ArH). $^{13}C\{^1H\}$ NMR ($CDCl_3$, 100.5 MHz): δ_C 26.7, 27.0, 101.6, 111.6, 117.9, 122.1, 124.0, 126.3, 127.5, 128.1, 128.5, 129.5, 129.8, 129.9, 130.9, 132.5, 132.6, 132.8, 133.2, 140.6, 143.6, 183.5, 185.1.

Platinacycle 17

Platinacycle 17 was prepared from 8 (50.0 mg, 0.055 mmol), acetylacetone (6.6 mg, 0.066 mmol) and K_2CO_3 (9.1 mg, 0.066 mmol) in acetonitrile (15 mL) and purified as described previously for platinacycle 10. The solid obtained after removal of the volatiles from the reaction mixture was dissolved in CH_2Cl_2 (2 mL), layered with toluene (2 mL) and stored at RT for 4 days to afford 17 as yellow crystals suitable for SCXRD. Yield = 84% (37.4 mg, 0.046 mmol). Mp: 244.9 °C. Anal. calcd for $C_{24}H_{20}Br_3N_3O_2Pt$ ($M_w = 813.88$): C, 35.27; H, 2.47; N, 5.14. Found: C, 35.48; H, 2.81; N, 5.47. ATR-IR (cm^{-1}): $\nu(N-H)$ 3350 (m); $\nu(C=N)$ 1626 (m); $\nu(C-O)$ (acac(1-)) 1574 (s); $\nu(C-O)$ (acac(1-)) 1520 (s). 1H NMR ($CDCl_3$, 400 MHz): δ_H 1.41, 1.88 (each s, $2 \times 3H$, CH_3 , acac(1-)), 5.26 (s, 1H, CH , acac(1-)), 5.95 (s, 1H, NH), 6.79 (t,

$J_{HH} = 7.6$ Hz, 1H, ArH), 7.14–7.20 (m, 3H, ArH), 7.36–7.48 (m, 4H, ArH (3H), NH (1H)), 7.65 (dt, $J_{HH} = 8.6$ Hz; 1.6 Hz, 3H, ArH), 7.75 (dd, $J_{HH} = 7.6$ Hz; 1.2 Hz, 1H, ArH). $^{13}C\{^1H\}$ NMR ($CDCl_3$, 100.5 MHz): δ_C 26.7, 27.1, 101.6, 108.6, 111.7, 120.5, 122.6, 123.3, 127.2, 127.3, 128.1, 128.3, 128.6, 129.3, 129.9, 133.0, 133.3, 133.5, 134.1, 134.4, 142.0, 143.9, 183.5, 185.1.

Platinacycle 18

Platinacycle 18 was prepared from 9 (50.0 mg, 0.069 mmol), acetylacetone (8.2 mg, 0.082 mmol) and K_2CO_3 (11.3 mg, 0.082 mmol) in acetonitrile (15 mL) and purified as described previously for platinacycle 10. The solid obtained after removal of the volatiles from the reaction mixture was dissolved in CH_2Cl_2 (2 mL), layered with toluene (2 mL) and stored at RT for 3 days to afford 18 as yellow crystals suitable for SCXRD. Yield = 86% (37.4 mg, 0.059 mmol). Mp: 260.1 °C. Anal. calcd for $C_{24}H_{20}F_3O_2N_3Pt$ ($M_w = 634.52$): C, 45.43; H, 3.18; N, 6.62. Found: C, 45.63; H, 3.33; N, 7.01. ATR-IR (cm^{-1}): $\nu(N-H)$ 3404.36 (m); $\nu(C=N)$ 1624 (m); $\nu(C-O)$ (acac(1-)) 1578 (s); $\nu(C-O)$ (acac(1-)) 1503 (s). ESI mass (HRMS) m/z [ion] calcd: 635.1234 $[M + H]^+$. Found: 635.1298. Platinacycle 18 exists in two isomeric forms with their approximate ratios being 1 : 0.07 as estimated from integrals of methyl protons of the acac(1-) ligand. 1H NMR ($CDCl_3$, 400 MHz): δ_H 1.46 (s, $2 \times 3H$, CH_3 , acac(1-), isomers 1 & 2), 1.87 (s, 3H, CH_3 , acac(1-), isomer 2), 1.89 (s, 3H, CH_3 , acac(1-), isomer 1), 5.26 (s, 1H, CH , acac(1-), isomer 2), 5.27 (s, 1H, CH , acac(1-), isomer 1), 5.84 (s, $2 \times 1H$, NH , isomers 1 & 2), 6.30 (dd, $J_{HH} = 8.6$ Hz; 5.0 Hz, $2 \times 1H$, ArH , isomers 1 & 2), 6.43 (s, $2 \times 1H$, NH , isomers 1 & 2), 6.63 (dt, $J_{HH} = 7.6$ Hz; 2.9 Hz, $2 \times 1H$, ArH , isomers 1 & 2), 7.06–7.14 (m, $2 \times 6H$, ArH , isomers 1 & 2), 7.25–7.28 (m, $2 \times 2H$, ArH , isomers 1 & 2), 7.45 (dd, $J_{HH} = 10.8$ Hz; 3.0 Hz, $2 \times 1H$, ArH , isomers 1 & 2). $^{13}C\{^1H\}$ NMR ($CDCl_3$, 100.5 MHz): δ_C 27.1, 101.7, 110.0 (d, $J_{C-F} = 24.1$ Hz), 112.2 (d, $J_{C-F} = 5.7$ Hz), 114.2 (d, $J_{C-F} = 7.7$ Hz), 115.8 (d, $J_{C-F} = 22.1$ Hz), 117.4 (d, $J_{C-F} = 22.2$ Hz), 119.6 (d, $J_{C-F} = 19.3$ Hz), 127.9 (d, $J_{C-F} = 8.6$ Hz), 129.7 (d, $J_{C-F} = 8.6$ Hz), 132.0, 133.8, 139.2, 145.1, 157.3 (d, $J_{C-F} = 241.7$ Hz), 160.2 (d, $J_{C-F} = 42.4$ Hz), 162.6 (d, $J_{C-F} = 45.3$ Hz), 183.6, 185.2. $^{19}F\{^1H\}$ NMR ($CDCl_3$, 376.31 MHz): δ_F -121.4 (isomers 1 & 2), -115.8 (isomer 2), -115.6 (isomer 1), -113.1 (isomer 2), -112.9 (isomer 1).

Platinacycle 19

Platinacycle 19 was prepared from 1 (50.0 mg, 0.073 mmol), 2-picolinic acid (10.8 mg, 0.088 mmol) and K_2CO_3 (12.1 mg, 0.088 mmol) in acetonitrile (15 mL) and purified as described previously for platinacycle 10. The solid obtained after removal of the volatiles from the reaction mixture was dissolved in CH_2Cl_2 (2 mL), layered with toluene (2 mL) and stored at RT for 2 days to afford 19 as green crystals suitable for SCXRD. Yield = 89% (45.1 mg, 0.065 mmol). Mp: 248.3 °C. Anal. calcd for $C_{28}H_{26}O_5N_4Pt$ ($M_w = 693.62$): C, 48.49; H, 3.78; N, 8.08. Found: C, 48.44; H, 3.68; N, 7.96. ATR-IR (cm^{-1}): $\nu(N-H)$ 3385 (m), $\nu(>C=O)$ 1657 (s), $\nu(C=N)$ 1611 (m). ESI mass (HRMS) m/z [ion]: calcd: 694.1629 $[M + H]^+$, Found: 694.1670; calcd: 1387.3237 $\{[Pt(TAG)(\mu_2-N,O-pic)]_2 + H\}$, Found: 1387.3265. 1H NMR ($CDCl_3$, 400 MHz): δ_H 3.80, 3.82, 4.02 (each s, $3 \times 3H$, OCH_3), 6.68 (d, $J_{HH} = 8.4$ Hz, 1H, ArH), 6.90–7.06 (m, 6H, ArH), 7.11–7.23 (m, 4H,



ArH), 7.27–7.33 (m, 2H, ArH), 7.87 (s, 1H, NH), 7.89–7.96 (m, 2H, ArH (1H), NH (1H)), 8.72 (d, $J_{\text{HH}} = 5.6$ Hz, 1H, ArH). $^{13}\text{C}\{^1\text{H}\}$ NMR (CDCl_3 , 100.5 MHz): δ_{C} 55.4, 55.9, 56.6, 105.5, 111.6, 112.7, 117.3, 120.9, 121.5, 122.4, 123.5, 126.0, 126.5, 126.9, 127.4, 128.0, 128.2, 129.4, 129.6, 133.6, 137.5, 145.8, 147.8, 148.9, 151.3, 154.0, 154.5, 172.3.

Author contributions

Project conceptualization, secured funding and supervision (NT), syntheses, characterization including SCXRD (VT), emission measurements (MA), emission data analyses (GVP), DFT and TD-DFT calculations (JMT), DFT and TD-DFT analyses (CS). The manuscript was written with contributions from all authors.

Conflicts of interest

There is no conflicts to declare.

Acknowledgements

We acknowledge SERB for research grant (EMR/2014/000698) and one of us (V. T.) acknowledges UGC for a fellowship. University Science Instrumentation Center, University of Delhi is acknowledged for infrastructural facilities. We thank Dr Nitish Kumar Sinha for some experimental assistance related to complexes **6** and **13**·0.5 toluene.

References

- (a) J. A. Gareth Williams, S. Develay, D. L. Rochester and L. Murphy, *Coord. Chem. Rev.*, 2008, **252**, 2596–2611; (b) J. Kalinowski, V. Fattori, M. Cocchi and J. A. Gareth Williams, *Coord. Chem. Rev.*, 2011, **255**, 2401–2425; (c) X. Yang, C. Yao and G. Zhou, *Platinum Met. Rev.*, 2013, **57**, 2–16; (d) T. Fleetham and J. Li, *J. Photonics Energy*, 2014, **4**, 040991; (e) S. Huo, J. Carroll and D. A. K. Vezzu, *Asian J. Org. Chem.*, 2015, **4**, 1210–1245; (f) K. Li, G. S. Ming Tong, Q. Wan, G. Cheng, W.-Y. Tong, W.-H. Ang, W.-L. Kwong and C.-M. Che, *Chem. Sci.*, 2016, **7**, 1653–1673; (g) C. Cebrián and M. Mauro, *Beilstein J. Org. Chem.*, 2018, **14**, 1459–1481; (h) X. Wang and S. Wang, *Chem. Rec.*, 2019, **19**, 1693–1709; (i) J. Herberger and R. F. Winter, *Coord. Chem. Rev.*, 2019, **400**, 213048; (j) A. Haque, H. El Moll, K. M. Alenezi, M. S. Khan and W.-Y. Wong, *Materials*, 2021, **14**, 4236.
- J. Brooks, Y. Babayan, S. Lamansky, P. I. Djurovich, I. Tsyba, R. Bau and M. E. Thompson, *Inorg. Chem.*, 2002, **41**, 3055–3066.
- J. C.-H. Chan, W. H. Lam, H.-L. Wong, N. Zhu, W.-T. Wong and V. W.-W. Yam, *J. Am. Chem. Soc.*, 2011, **133**, 12690–12705.
- D. N. Kozhevnikov, V. N. Kozhevnikov, M. M. Ustinova, A. Santoro, D. W. Bruce, B. Koenig, R. Czerwieniec, T. Fischer, M. Zabel and H. Yersin, *Inorg. Chem.*, 2009, **48**, 4179–4189.
- A. Bossi, A. F. Rausch, M. J. Leitl, R. Czerwieniec, M. T. Whited, P. I. Djurovich, H. Yersin and M. E. Thompson, *Inorg. Chem.*, 2013, **52**, 12403–12415.
- O. J. Stacey, B. D. Ward, S. J. Coles, P. N. Horton and S. J. A. Pope, *Dalton Trans.*, 2016, **45**, 10297–10307.
- M. Z. Shafikov, D. N. Kozhevnikov, M. Bodensteiner, F. Brandl and R. Czerwieniec, *Inorg. Chem.*, 2016, **55**, 7457–7466.
- Y.-J. Cho, S.-Y. Kim, H.-J. Son, D. W. Cho and S. O. Kang, *Phys. Chem. Chem. Phys.*, 2017, **19**, 5486–5494.
- N. Okamura, T. Maeda, H. Fujiwara, A. Soman, K. N. Narayanan Unni, A. Ajayaghosh and S. Yagi, *Phys. Chem. Chem. Phys.*, 2018, **20**, 542–552.
- Y. Zhou, J. Jia, L. Cai and Y. Huang, *Dalton Trans.*, 2018, **47**, 693–699.
- P.-H. Lanoë, A. Moreno-Betancourt, L. Wilson, C. Philouze, C. Monnereau, H. Jamet, D. Jouvenot and F. Loiseau, *Dyes Pigm.*, 2019, **162**, 967–977.
- A. F. Henwood, J. Webster, D. Cordes, A. M. Z. Slawin, D. Jacquemin and E. Zysman-Colman, *RSC Adv.*, 2017, **7**, 25566–25574.
- (a) X. Mou, Y. Wu, S. Liu, M. Shi, X. Liu, C. Wang, S. Sun, Q. Zhao, X. Zhou and W. Huang, *J. Mater. Chem.*, 2011, **21**, 13951–13962; (b) C.-H. Chen, F.-I. Wu, Y.-Y. Tsai and C.-H. Cheng, *Adv. Funct. Mater.*, 2011, **21**, 3150–3158.
- W. Zeng, M.-J. Sun, Z.-L. Gong, J.-Y. Shao, Y.-W. Zhong and J. Yao, *Inorg. Chem.*, 2020, **59**, 11316–11328.
- (a) K. Venkatesan, P. H. J. Kouwer, S. Yagi, P. Müller and T. M. Swager, *J. Mater. Chem.*, 2008, **18**, 400–407; (b) A. Santoro, A. C. Whitwood, J. A. Gareth Williams, V. N. Kozhevnikov and D. W. Bruce, *Chem. Mater.*, 2009, **21**, 3871–3882; (c) T. Sato, H. Awano, O. Haba, H. Katagiri, Y.-J. Pu, T. Takahashi and K. Yonetake, *Dalton Trans.*, 2012, **41**, 8379–8389; (d) M. Spencer, A. Santoro, G. R. Freeman, Á. Diez, P. R. Murray, J. Torroba, A. C. Whitwood, L. J. Yellowlees, J. A. Gareth Williams and D. W. Bruce, *Dalton Trans.*, 2012, **41**, 14244–14256.
- W. Wu, C. Cheng, W. Wu, H. Guo, S. Ji, P. Song, K. Han, J. Zhao, X. Zhang, Y. Wu and G. Du, *Eur. J. Inorg. Chem.*, 2010, **2010**, 4683–4696.
- C. Liu, X. Song, Z. Wang and J. Qiu, *ChemPlusChem*, 2014, **79**, 1472–1481.
- C. Liu, X. Song, X. Rao, Y. Xing, Z. Wang, J. Zhao and J. Qiu, *Dyes Pigm.*, 2014, **101**, 85–92.
- (a) Y. Xing, C. Liu, J.-H. Xiu and J.-Y. Li, *Inorg. Chem.*, 2015, **54**, 7783–7790; (b) Y. Xing, C. Liu, X. Song and J. Li, *J. Mater. Chem. C*, 2015, **3**, 2166–2174.
- A. S. Ionkin, W. J. Marshall and Y. Wang, *Organometallics*, 2005, **24**, 619–627.
- H. Li, W. Yuan, X. Wang, H. Zhan, Z. Xie and Y. Cheng, *J. Mater. Chem. C*, 2015, **3**, 2744–2750.
- A. Heil and C. M. Marian, *Inorg. Chem.*, 2019, **58**, 6123–6136.
- Z. M. Hudson, C. Sun, M. G. Helander, Y.-L. Chang, Z.-H. Lu and S. Wang, *J. Am. Chem. Soc.*, 2012, **134**, 13930–13933.
- T. Strassner, *Acc. Chem. Res.*, 2016, **49**, 2680–2689.
- M. Micksch, M. Tenne and T. Strassner, *Organometallics*, 2014, **33**, 3464–3473.



- 26 W. Wu, H. Guo, W. Wu, S. Ji and J. Zhao, *Inorg. Chem.*, 2011, **50**, 11446–11460.
- 27 A. Caubet, C. Lopez, X. Solans and M. Font-Bardia, *J. Organomet. Chem.*, 2003, **669**, 164–171.
- 28 Y. Yu, Scaffidi-Domianello, A. A. Nazarov, M. Haukka, M. Galanski, B. K. Keppler, J. Schneider, P. Du, R. Eisenberg and V. Yu. Kukushkin, *Inorg. Chem.*, 2007, **46**, 4469–4482.
- 29 S. U. Pandya, K. C. Moss, M. R. Bryce, A. S. Batsanov, M. A. Fox, V. Jankus, H. A. Al Attar and A. P. Monkman, *Eur. J. Inorg. Chem.*, 2010, **2010**, 1963–1972.
- 30 P. Elumalai, N. Thirupathi and M. Nethaji, *Inorg. Chem.*, 2013, **52**, 1883–1894.
- 31 V. Mishra and N. Thirupathi, *ACS Omega*, 2018, **3**, 6075–6090.
- 32 N. K. Sinha, V. Mishra and N. Thirupathi, *Inorg. Chem.*, 2023, **62**, 7644–7661.
- 33 Z. M. Hudson, B. A. Blight and S. Wang, *Org. Lett.*, 2012, **14**, 1700–1703.
- 34 D. Poveda, A. Vivancos, D. Bautista and P. Gonzalez-Herrero, *Inorg. Chem.*, 2023, **62**, 6207–6213.
- 35 V. Thakur and N. Thirupathi, *J. Organomet. Chem.*, 2020, **911**, 121138.
- 36 R. Ujjval, M. Deepa, J. M. Thomas, C. Sivasankar and N. Thirupathi, *Organometallics*, 2020, **39**, 3663–3678.
- 37 V. Mishra, N. K. Sinha and N. Thirupathi, *Inorg. Chem.*, 2021, **60**, 3879–3892.
- 38 V. Thakur and N. Thirupathi, *J. Organomet. Chem.*, 2022, **959**, 122200.
- 39 (a) J. R. L. Priqueler, I. S. Butler and F. D. Rochon, *Appl. Spectrosc. Rev.*, 2006, **41**, 185–226; (b) B. M. Still, P. G. A. Kumar, J. R. Aldrich-Wright and W. S. Price, *Chem. Soc. Rev.*, 2007, **36**, 665–686.
- 40 O. J. Stacey, J. A. Platts, S. J. Coles, P. N. Horton and S. J. A. Pope, *Inorg. Chem.*, 2015, **54**, 6528–6536.
- 41 J. A. Lowe, O. J. Stacey, P. N. Horton, S. J. Coles and S. J. A. Pope, *J. Organomet. Chem.*, 2016, **805**, 87–93.
- 42 E. Lindner, R. Fawzi, H. A. Mayer, K. Eichele and W. Hiller, *Organometallics*, 1992, **11**, 1033–1043.
- 43 S. Fuertes, A. J. Chueca and V. Sicilia, *Inorg. Chem.*, 2015, **54**, 9885–9895.
- 44 (a) M. Brookhart, M. L. H. Green and G. Parkin, *Proc. Natl. Acad. Sci. U.S.A.*, 2007, **104**, 6908–6914; (b) K. A. Siddiqui and E. R. T. Tiekink, *Chem. Commun.*, 2013, **49**, 8501–8503; (c) M. Baya, U. Belio and A. Martin, *Inorg. Chem.*, 2014, **53**, 189–200; (d) J. Kozelka, in *Noncovalent Forces*, ed. S. Scheiner, Springer International Publishing, Cham, 2015, vol. 19, pp. 129–158; (e) A. Pérez-Bitrián, M. Baya, J. M. Casas, A. Martín and B. Menjón, *Dalton Trans.*, 2021, **50**, 5465–5472.
- 45 L. Brammer, M. C. McCann, R. M. Bullock, R. K. McMullan and P. Sherwood, *Organometallics*, 1992, **11**, 2339–2341.
- 46 L. Brammer, J. M. Charnock, P. L. Goggin, R. J. Goodfellow, T. F. Koetzle and A. G. Orpen, *J. Chem. Soc., Chem. Commun.*, 1987, 443–445.
- 47 W. Yao, O. Eisenstein and R. H. Crabtree, *Inorg. Chim. Acta*, 1997, **254**, 105–111.
- 48 Y. Zhang, J. C. Lewis, R. G. Bergman, J. A. Ellman and E. Oldfield, *Organometallics*, 2006, **25**, 3515–3519.
- 49 Y. Unger, D. Meyer, O. Molt, C. Schildknecht, I. Munster, G. Wagenblast and T. Strassner, *Angew. Chem., Int. Ed.*, 2010, **49**, 10214–10216.
- 50 S. Stipurin, F. Wurl and T. Strassner, *Organometallics*, 2022, **41**, 313–320.
- 51 S. Poirier, F. Rahmani and C. Reber, *Dalton Trans.*, 2017, **46**, 5279–5287.
- 52 S. Poirier, H. Lynn, C. Reber, E. Tailleur, M. Marchivie, P. Guionneau and M. R. Probert, *Inorg. Chem.*, 2018, **57**, 7713–7723.
- 53 L. F. Gildea and J. A. Gareth Williams, Iridium and platinum complexes for OLEDs, in *Organic Light-Emitting Diodes: Materials, Devices and Applications*, ed. A. Buckley, Woodhead, Cambridge, 2013, pp. 77–113.
- 54 A. D. Becke, *Phys. Rev. A*, 1988, **38**, 3098–3100.
- 55 A. D. Becke, *J. Chem. Phys.*, 1993, **98**, 1372–1377.
- 56 A. D. Becke, *J. Chem. Phys.*, 1993, **98**, 5648–5652.
- 57 R. Krishnan, J. S. Binkley, R. Seeger and J. A. Pople, *J. Chem. Phys.*, 1980, **72**, 650–654.
- 58 T. H. Dunning Jr and P. J. Hay, in *Modern Theoretical Chemistry*, ed. H. F. Schaefer III, Plenum, New York, 1976.
- 59 P. J. Hay and W. R. Wadt, *J. Chem. Phys.*, 1985, **82**, 270–283.
- 60 P. J. Hay and W. R. Wadt, *J. Chem. Phys.*, 1985, **82**, 284–298.
- 61 P. J. Hay and W. R. Wadt, *J. Chem. Phys.*, 1985, **82**, 299–310.
- 62 M. T. Cancès, B. Mennucci and J. Tomasi, *J. Chem. Phys.*, 1997, **107**, 3032–3041.
- 63 M. Cossi, V. Barone, B. Mennucci and J. Tomasi, *Chem. Phys. Lett.*, 1998, **286**, 253–260.
- 64 B. Mennucci and J. Tomasi, *Chem. Phys.*, 1997, **106**, 5151–5158.
- 65 M. J. Frisch, G. W. Trucks, H. B. Schlegel, G. E. Scuseria, M. A. Robb, J. R. Cheeseman, J. A. Montgomery Jr, T. Vreven, K. N. Kudin, J. C. Burant, J. M. Millam, S. S. Iyengar, J. Tomasi, V. Barone, B. Mennucci, M. Cossi, G. Scalmani, N. Rega, G. A. Petersson, H. Nakatsuji, M. Hada, M. Ehara, K. Toyota, R. Fukuda, J. Hasegawa, M. Ishida, T. Nakajima, Y. Honda, O. Kitao, H. Nakai, M. Klene, X. Li, J. E. Knox, H. P. Hratchian, J. B. Cross, C. Adamo, J. Jaramillo, R. Gomperts, R. E. Stratmann, O. Yazyev, A. J. Austin, R. Cammi, C. Pomelli, J. W. Ochterski, P. Y. Ayala, K. Morokuma, G. A. Voth, P. Salvador, J. J. Dannenberg, V. G. Zakrzewski, S. Dapprich, A. D. Daniels, M. C. Strain, O. Farkas, D. K. Malick, A. D. Rabuck, K. Raghavachari, J. B. Foresman, J. V. Ortiz, Q. Cui, A. G. Baboul, S. Clifford, J. Cioslowski, B. B. Stefanov, G. Liu, A. Liashenko, P. Piskorz, I. Komaromi, R. L. Martin, D. J. Fox, T. Keith, M. A. Al-Laham, C. Y. Peng, A. Nanayakkara, M. Challacombe, P. M. W. Gill, B. Johnson, W. Chen, M. W. Wong, C. Gonzalez and J. A. Pople, *Gaussian 09, Rev. A.02*, Gaussian, Inc., Wallingford CT, 2009.

